1up

NASA CR 114571

AVAILABLE TO THE PUBLIC

EFFECT OF CROSSFLOW VELOCITY ON
THE GENERATION OF LIFT FAN
JET NOISE IN VTOL
AIRCRAFT

D.L. Stimpert
R.G. Fogg

GENERAL ELECTRIC COMPANY

prepared for

NATIONAL AERONAUTICS AND SPACE ADMINISTRATION

NASA- Ames Research Center

Contract NAS2 - 5462

D.H. Hickey - Project Manager

43

1. Report No. NASA CR 114571	2. Government Accession No.	3. Recipient's Catalog No.
4. Title and Subtitle Effect of Crossflow Velocity on the Generation of Lift Fan Jet Noise in VTOL Aircraft		5. Report Date February 1973
		6. Performing Organization Code
7. Author(s) D.L. Stimpert, R.G. Fogg		8. Performing Organization Report No.
		10. Work Unit No.
9. Performing Organization Name and Address General Electric Company Aircraft Engine Group Cincinnati, Ohio 45215		11. Contract or Grant No. NAS2-5462
		13. Type of Report and Period Covered Contractor Report
12. Sponsoring Agency Name and Address National Aeronautics & Space Administration Washington, D.C. 20546		14. Sponsoring Agency Code
15. Supplementary Notes Project Manager, D.H. Hickey NASA Ames Research Center Moffett Field, California		

16. Abstract

Analytical studies based on a turbulent mixing noise prediction technique indicate that jet noise power levels are increased when a jet is situated in a crossflow. V/STOL model transport acoustic test data obtained in the NASA Ames 40' x 80' (12.2 m x 24.4 m) wind tunnel confirmed this jet noise power level increase due to crossflow. Increases up to 6 dB at a Strouhal number of 2.5 and crossflow velocity to jet velocity ratio of 0.58 were observed. The power level increases observed in the experimental data confirm the predicted power level increases.

17. Key Words (Suggested by Author(s))	18. Distribution Statement
Crossflow Velocity Jet Noise Lift Fan VTOL Aircraft	Unclassified - Unlimited

19. Security Classif. (of this report)	20. Security Classif. (of this page)	21. No. of Pages	22. Price*
Unclassified	Unclassified	36	

* For sale by the National Technical Information Service, Springfield, Virginia 22151

FOREWORD

The authors wish to acknowledge the cooperation of D. Hickey, J. Kirk and A. Atencio of NASA Ames in making available the data sources used in the experimental analysis portion of this report.

TABLE OF CONTENTS

	Page
FOREWORD	ii
LIST OF FIGURES	iv
SYMBOLS	vi
SUMMARY	1
INTRODUCTION	2
ANALYTICAL STUDY	3
Crosswind Adjustment to Jet Noise	
EXPERIMENTAL ANALYSIS	6
V/STOL Model and Data Acquisition	
Lift/Cruise Fans	
Lift Fans	
COMPARISON OF ANALYTICAL AND EXPERIMENTAL RESULTS	9
CONCLUSIONS	10
FIGURES	11
REFERENCES	36

LIST OF FIGURES

Figure		Page
1.	Schematic of Jet in Crossflow	11
2.	Predicted Power Spectra Change for Jets in Crossflow	12
3.	Microphone and V/STOL Model Transport Location in Ames Wind Tunnel	13
4.	V/STOL Model Transport Schematic	14
5.	Effect of Crossflow on 50 Hz SPL of V/STOL Model Lift/Cruise Fans (Downstream Microphones)	15
6.	Effect of Crossflow on 50 Hz SPL of V/STOL Model Lift/Cruise Fans (Upstream Microphones)	16
7.	Effect of Crossflow on 100 Hz SPL of V/STOL Model Lift/Cruise Fans (Downstream Microphones)	17
8.	Effect of Crossflow on 100 Hz SPL of V/STOL Model Lift/Cruise Fans (Upstream Microphones)	18
9.	Effect of Crossflow on 200 Hz SPL of V/STOL Model Lift/Cruise Fans (Downstream Microphones)	19
10.	Effect of Crossflow on 200 Hz SPL of V/STOL Model Lift/Cruise Fans (Upstream Microphones)	20
11.	Effect of Crossflow on 400 Hz SPL of V/STOL Model Lift/Cruise Fans (Downstream Microphones)	21
12.	Effect of Crossflow on 400 Hz SPL of V/STOL Model Lift/Cruise Fans (Upstream Microphones)	22
13.	Effect of Crossflow on 800 Hz SPL of V/STOL Model Lift/Cruise Fans (Downstream Microphones)	23
14.	Effect of Crossflow on 800 Hz SPL of V/STOL Model Lift/Cruise Fans (Upstream Microphones)	24
15.	V/STOL Model Lift/Cruise Fan Jet Noise Directivity Pattern at Vo/Vjet = 0 and 0.396	25
16.	V/STOL Model Lift/Cruise Fan Jet Noise Directivity Pattern at Vo/Vjet = 0 and 0.396	26

LIST OF FIGURES - Concluded

Figure		Page
17.	Jet Noise Power Level Increase with Increased Crossflow at Various Strouhal Numbers	27
18.	Jet Noise Power Level Change as a Function of Strouhal Number for Various Crossflow Velocity Ratios	28
19.	Effect of Crossflow on 100 Hz Signal from V/STOL Model Lift Fans (Downstream Microphones)	29
20.	Effect of Crossflow on 100 Hz Signal from V/STOL Model Lift Fans (Upstream Microphones)	30
21.	V/STOL Model Lift Fan Jet Noise Directivity Pattern at 100 Hz	31
22.	Comparison of Crossflow Effect on Jet Noise Power Level of V/STOL Model Lift Fans and Lift/Cruise Fans	32
23.	Comparison of Measured and Predicted Power Spectra at Vo/Vjet = 0.091	33
24.	Comparison of Measured and Predicted Power Spectra at Vo/Vjet = 0.2	34
25.	Comparison of Measured and Predicted Power Spectra at Vo/Vjet = 0.33	35

SYMBOLS

		Units	
$A(y)$	Jet area	FT^2	m^2
d_j	Diameter of jet at exit plane	FT	m
f	Frequency	Hz	
K_1	Empirical constant		
K_2	Empirical constant		
P	Power	watts	
PWL	Sound Power Level Re 10^{-13} watts	dB	
r	Radius	FT	m
S_n	Strouhal number, fd_j/V_{jet}		
SPL	Sound pressure level Re 0.0002 microbar	dB	
V	Jet Velocity	FT/sec	m/sec
V_{jet}	Jet Exit Velocity	FT/sec	m/sec
$V(X,Y)$	Velocity distribution in a plane perpendicular to the jet trajectory axis	FT/sec	m/sec
V_o	Crossflow velocity	FT/sec	m/sec
V_r	Relative velocity	FT/sec	m/sec
x	Space coordinate parallel to crossflow velocity in jet exhaust plane	FT	m
X	Space coordinate in a plane perpendicular to the jet axis	FT	m
y	Space coordinate parallel to jet exhaust velocity at jet exhaust plane	FT	m
Y	Space coordinate in a plane perpendicular to the jet axis	FT	m
α	Jet trajectory slope, dy/dx	Degrees	
α_1	V/STOL model transport yaw angle	Degrees	
β_V	Exhaust louver angle of V/STOL model lift fans	Degrees	
σ_{CN}	V/STOL model transport lift/cruise nozzle exhaust exit angle	Degrees	
ξ	Jet trajectory coordinate	FT	m

SUMMARY

Possible installations for lift fans in future V/STOL aircraft include vertical mounting in wing pods, vertical mounting in the fuselage, and lift-cruise mounting on the fuselage with the jet being vectored for lift and cruise. In all these possible configurations, the jet will experience various degrees of crossflow during flight. An investigation was conducted into the effects of crossflow velocity on the generation of lift fan jet noise. This investigation included an analytical study and an examination of experimental data, both of which confirmed an increase in jet noise sound power level with increasing crossflow velocities. The aero-acoustic analysis utilized a turbulent mixing noise prediction technique which is based upon a velocity profile method that was modified to handle deflected jet velocity profiles. Confirmation of the aero-acoustic analysis was obtained by examining acoustic data recorded during testing of a V/STOL model in the NASA Ames 40 foot by 80 foot (12.2m by 24.4m) wind tunnel.

INTRODUCTION

Research is currently being directed toward the design of V/STOL aircraft to be used as commercial subsonic transports. Many of the configurations being considered by NASA and the airframe manufacturers incorporate lift fans which are fixed in wing pods or mounted in the fuselage with the inlets oriented vertically. During transition from vertical to horizontal flight on takeoff or the reverse on landing, exhaust jets from these lift fans experience various degrees of crossflow velocities.

During aerodynamic and acoustic investigations of a large scale lift fan model in the NASA Ames 40' by 80' (12.2m x 24.4m) wind tunnel, sound pressure levels in the jet noise region of the spectrum were observed to increase when the jet was issuing perpendicular to the crossflow (Reference 1). This paper reports on analysis of additional noise measurements taken in the NASA Ames 40' by 80' (12.2m by 24.4m) wind tunnel with a complete lift fan aircraft model. The results were analyzed to give an empirical understanding of jet noise in a crossflow and to provide verification of an analytical study.

ANALYTICAL STUDY

CROSS WIND ADJUSTMENT TO JET NOISE

The jet noise adjustment used in the prediction model to account for introducing a cross wind component to the jet flow is based on several fundamental theoretical noise relationships with modifying assumptions. This cross wind adjustment factor is applied to the undisturbed jet noise spectra to arrive at a predicted jet noise with cross wind.

The reference jet noise spectra is prepared using the method delineated in Reference 2. The flight Strouhal curve is used as being representative of the free field sound generating conditions experienced in aircraft flyover. This jet noise spectra is calculated for a jet exhausting into an undisturbed area with the assumption that complete mixing occurs between the fan and jet stream so that the characteristics of a single jet stream are used to obtain the jet spectra.

The evaluation of the acoustic power spectra of a jet in a crossflow is based on a turbulent mixing noise analysis using a velocity profile method as outlined in Reference 3. To compute the acoustic quantities two basic assumptions are employed:

1. For static jets or jets without crossflow, the sound power, P, generated by a slice of a circular jet obeys Lighthill's eighth power law

$$\frac{dP}{dy} \sim \int_{A(y)} V^8 \, dA \qquad (1)$$

where V is the mean velocity which varies with axial location y and radial distance r from the jet centerline and A (y) is the cross section area of the jet at the axial location y.

2. The nomdimensional sound frequency (Reference 3 and 4) is directly proportional to nondimensional axial location as defined by the empirical relationship

$$\frac{fd_j}{V_{jet}} = (K_1 \, y/d_j)^{-K_2} \qquad (2)$$

where f is the frequency, d_j the jet exit diameter, V_{jet} the jet exit velocity, and K_1 and K_2 are experimentally determined constants which have values of 1.25 and 1.22 respectively.

To evaluate equation 1, the velocity profiles at each axial location are needed. In this way, the power per slice of jet can be readily converted to a power per frequency band (or power spectral level). For a jet in a crossflow, the trajectory, jet spread, and velocity profiles are computed from the model of Bowley and Sucec in Reference 5. Their analysis treats the deflected jet as a jet composed of two regions - an initial mixing region and a fully mixed region. Figure 1 presents the coordinates and form of the deflected jet characteristics.

Acoustically, the splitting of the jet into two aerodynamic regions also splits the acoustic analysis represented by equation 1 into two regions. There is a high frequency region associated with the initial mixing region and a low frequency region associated with the fully mixed region of the deflected jet. The superposition of these regions results in the total power of the jet.

The frequency location along the axis of the deflected jet is represented by equation 2 where the axial location y for a static jet is replaced by the deflected jet trajectory location ξ; therefore equation 2 becomes

$$\frac{fd_j}{V_{jet}} = (K_1 \quad \xi/d_j)^{-K_2} \tag{3}$$

By assuming that the static velocity profiles in equation 1 may be replaced by relative velocity profiles of a deflected jet or

$$V_R = V \ (X,Y) - V_o \cos \alpha \tag{4}$$

a complete computational system is set for calculating the power spectral properties of a jet in a crossflow. In equation 4, V_R is the relative velocity, V (X,Y) is the velocity in a plane perpendicular to the deflected jet axis, V_o is the crossflow velocity, and α is the jet trajectory slope. As in Reference 5, the shape of the jet in a plane perpendicular to the deflected jet axis is assumed rectangular. Typical results of these calculations are shown on Figure 2 with the peak sound power level occurring at the transition point between the initial mixing region and the fully mixed region. For $V_o/V_{jet} = 0$, the spectra correspond to those predicted by reference 2. This sound power level increment in decibels is assumed equal to the sound pressure level change. Since this increment is based on the SAE reference acoustic angle of 135°, the increment is allocated to all acoustic angles using a jet spectra directivity factor currently in use accounting for the deflection angle for each frequency. Consequently, the result of the calculation is a noise spectra in units of SPL for all frequencies and acoustic angles adjusted for cross wind effects.

Preliminary analysis of predicted power level spectra had indicated a crossover or decrease in power level at high frequencies as crosswind increased. This was not consistent with experimental data (see Section IV) and a modification to the method of reference 5 was made. This modification assumed no deflection of the jet axis in the initial region or more specifically the deflection angle $\alpha = 90°$ and $\cos \alpha = 0$. Consequently, on the power frequency plot presented in Figure 2, the lines representing varying cross flow strengths are regular without any crossover in the range of frequencies generated in the initial region. It is noted, however, that the transition point on the jet axis between the initial and turbulent region still varies as a function of crossflow strength.

EXPERIMENTAL ANALYSIS

V/STOL Model and Data Acquisition

A scale model aircraft configured as a V/STOL transport was tested in the 40' x 80' (12.2 m x 24.4 m) wind tunnel at NASA Ames. The aircraft had four X376B fans of which two were mounted in deep inlets in the nose and two were mounted as lift/cruise fans near the tail. The exhaust of the lift/cruise fans could be vectored downward simulating a lift mode. Exhaust from a T58 gas generator drove the tip turbine of each 36 inch (.914 m) diameter fan. Each fan had a design pressure ratio of 1.08 and a tip speed of 640 feet per second (195 m/ sec). Figure 3 identifies the fan locations on the model and the microphone locations in the wind tunnel, while Figure 4 is a schematic of the V/STOL model transport.

Noise measurements were recorded on magnetic tape at various tunnel speeds for various combinations of lift fans and lift/cruise fans in operation by NASA Ames personnel. The data were processed at General Electric Edwards Flight Test Center to give 1/3 octave band sound pressure levels at each microphone for each test point. All data for this report were referenced to a 120 foot (36.5 m) radius by extrapolating the SPL's measured at each microphone under the assumption of spherical divergence. No corrections for tunnel reverberation effects are included in the data.

Lift/Cruise Fans

To understand the effect of crossflow on jet noise, data from runs with the lift/cruise exhaust nozzle in the lift mode (δ_{CN} = 90°) were analyzed for various tunnel speeds. Figures 5 through 14 show the effect of crossflow velocity (expressed here as the ratio of tunnel velocity to jet exit velocity) on 1/3 octave band sound pressure levels at all microphones and at frequencies of 50, 100, 200, 400 and 800 Hz. It should be noted that the levels measured are above the tunnel "floor" or background noise. Reference 6 indicates that the tunnel broadband noise floor is on the order of 80 dB up to velocity ratios of 0.4. As tunnel velocity and therefore crossflow velocity ratio decreases, the tunnel noise floor which is broadband in nature drops accordingly. Reference 6 places the broadband floor at low tunnel speeds at 65 dB ± 5 dB.

There is a definite increase due to crossflow indicated for all microphones up to and including 400 Hz. 800 Hz data show only a slight increase in SPL as crossflow velocity increases. For this frequency and presumably higher frequencies, the noise may be dominated by fan broadband noise. Reference 7 has shown that the fan pure tone noise of the lift/cruise fans does not increase with increasing tunnel velocity since the fan inlet is aligned with the flow and does not experience a true crossflow. Assuming that the fan broadband noise follows the same trend and that fan broadband noise is dominant at 800 Hz would account for the data of Figures 13 and 14. The downstream microphones (numbers 1 through 5) at 50 Hz exhibit large change in SPL with crossflow. Whether this is an actual increase due to crossflow or the result of inaccuracies involved in measuring low frequency noise is not certain at this time.

The data of Figures 4 through 14 were used to determine the change in jet noise at selected crossflow velocity ratios for five 1/3 octave bands (50, 100, 200, 400, and 800 Hz). The procedure is demonstrated for a crossflow velocity ratio of 0.396. Shown in Figures 15 and 16 are plots of 1/3 octave band SPL at frequencies of 50, 100, 200, 400, and 800 Hz both with and without crossflow. The acoustic angles for each microphone were calculated relative to the lift/cruise fan exhaust axis. At each frequency, there is a change due to crossflow which is approximately constant for all angles. This means that one can assume that the power level change due to crossflow is equal to the measured SPL change. With the exception of the 50 Hz data in Figure 15, upstream and downstream microphones show the same increase with crossflow.

Similar analysis at velocity ratios of 0.175 generated the curves shown on Figure 17 which are the power level changes due to an increase in crossflow velocity at five frequencies. Each frequency was normalized to a Strouhal number ($S_n = \frac{f\, d_j}{V_{jet}}$).

Figure 18 was generated by reading the ΔPWL values of the lines drawn through the data of Figure 16 and represents the measured power level increase as a function of Strouhal number for various crossflow to jet velocity ratios.

Lift Fans

Another source of jet noise data was noise measurements taken with the forward lift fans of the V/STOL model in operation at various tunnel speeds. The data were evaluated in the same manner as the lift/cruise fans. Figures 19 and 20 show the change in 100 Hz 1/3 octave band sound pressure level for increasing crossflow. To date, only the 100 Hz data has been analyzed. After calculating the acoustic angle "seen" by each microphone relative to the exhaust axis of lift fan number one, the plots of Figure 21 were made. The data points represent the value of the lines through the data of Figures 19 and 20 read at the corresponding crossflow ratio. For each crossflow ratio, there is an SPL increase which is constant over all acoustic angles. As a result, one can assume that the jet noise power level increase is identical to the SPL increase. Figure 22 compares the jet noise power level increase indicated by the lift fan data of Figure 21 with the lift/cruise results obtained by reading Figure 18 at $S_n = 1.82$. The resulting comparison is good although the forward lift fan increase at this selected frequency is higher than that of the lift/cruise fans.

COMPARISON OF THEORETICAL AND EXPERIMENTAL RESULTS

Figures 23, 24, and 25 represent a comparison of the analytical and experimental results of the lift/cruise fans. For these comparisons at three crossflow velocity ratios, the experimental incremental change in power level from Figure 18 was added to the zero crossflow curve of Figure 2. The resulting comparisons indicate that the predicted power level increase and experimental increase due to increasing crossflow are in good agreement.

CONCLUSIONS

This investigation included both an analytical study and an examination of experimental data to determine the effect of crossflow velocity on the jet noise generation of lift fans. It was found that an increase in jet noise power level is associated with an increase in crossflow velocity perpendicular to the jet exhaust axis. This predicted increase is confirmed by experimental data from wind tunnel tests of a V/STOL model. It is recommended that the analytically predicted jet noise power levels with crossflow effects be incorporated into current prediction techniques.

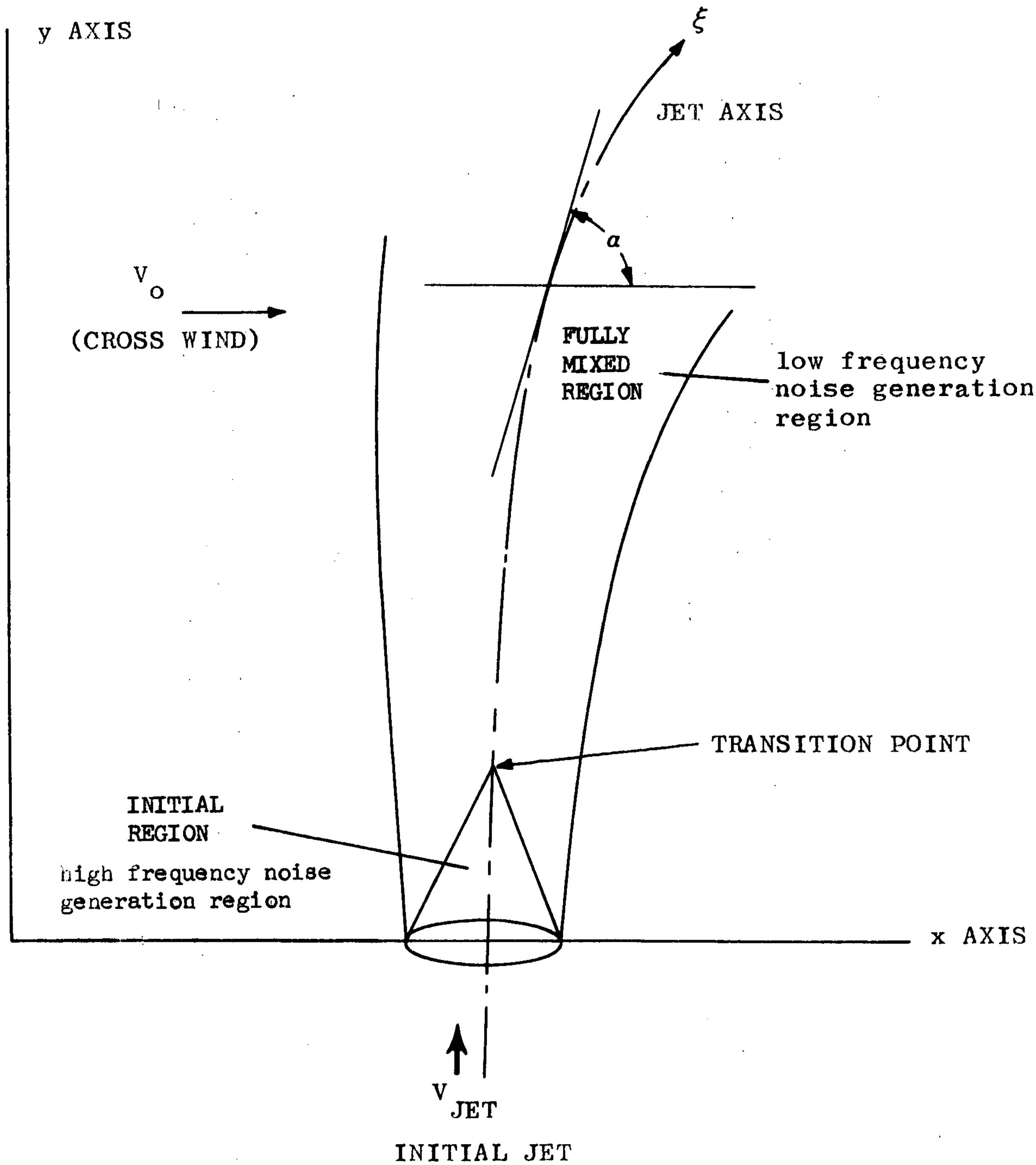

FIGURE 1 SCHEMATIC OF JET IN CROSS FLOW

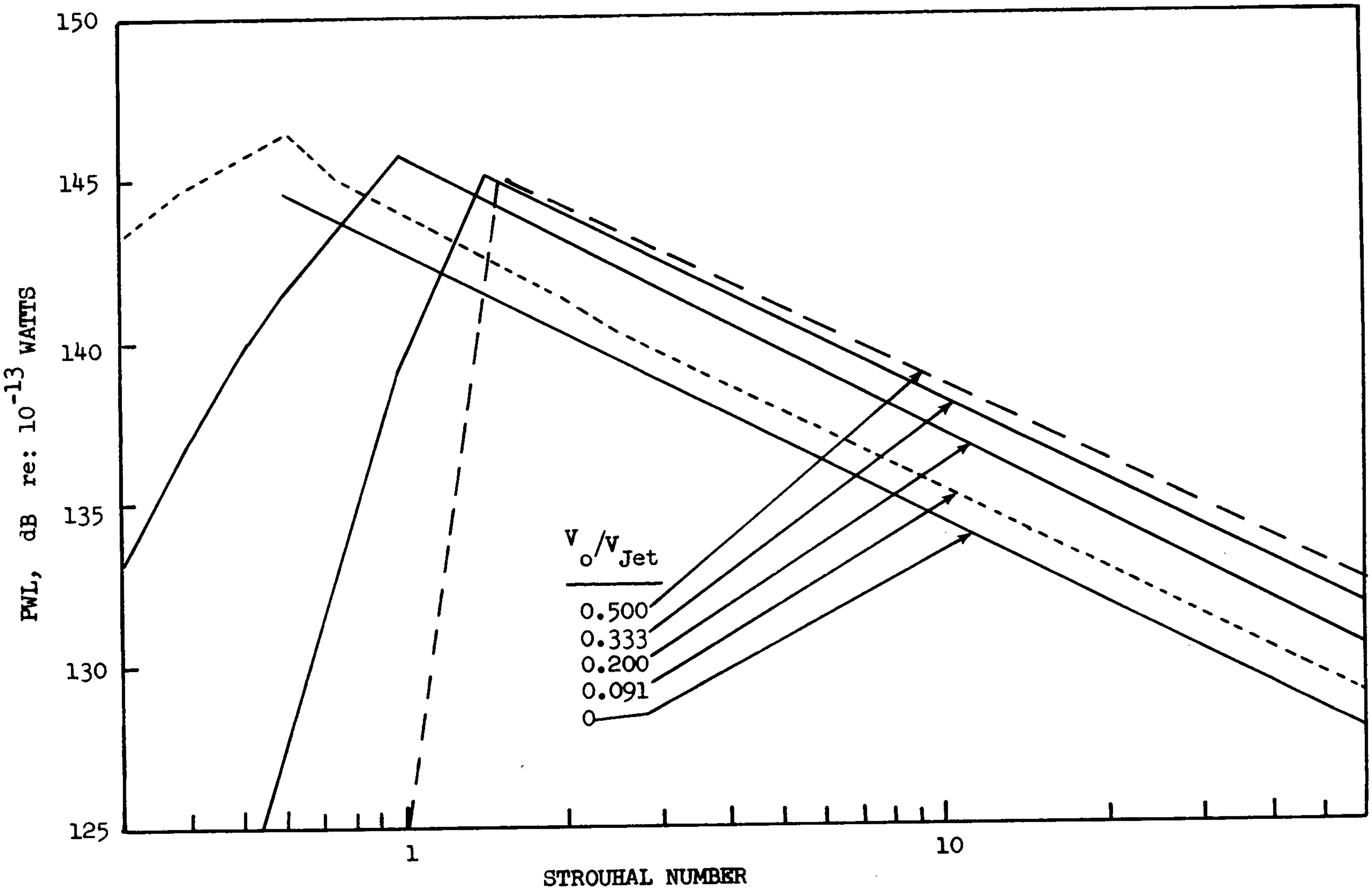

FIGURE 2 PREDICTED POWER SPECTRA CHANGE FOR JETS IN CROSSFLOW.

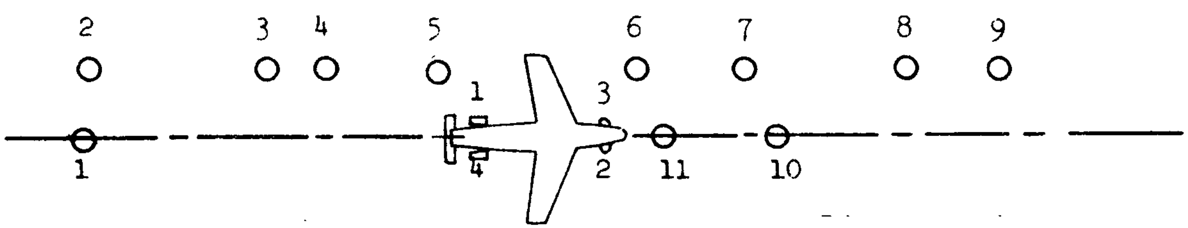

ENGINE LOCATION

1 & 2 LIFT ENGINES

3 & 4 CRUISE ENGINES (CAN BE VECTORED FOR LIFT)

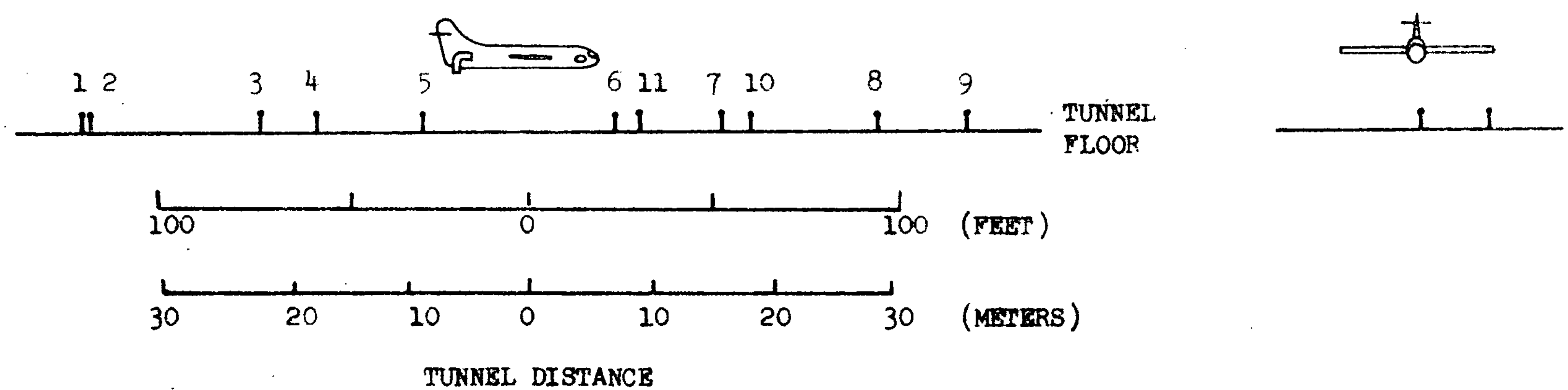

FIGURE 3 MICROPHONE AND V/STOL MODEL TRANSPORT LOCATION IN AMES WIND TUNNEL.

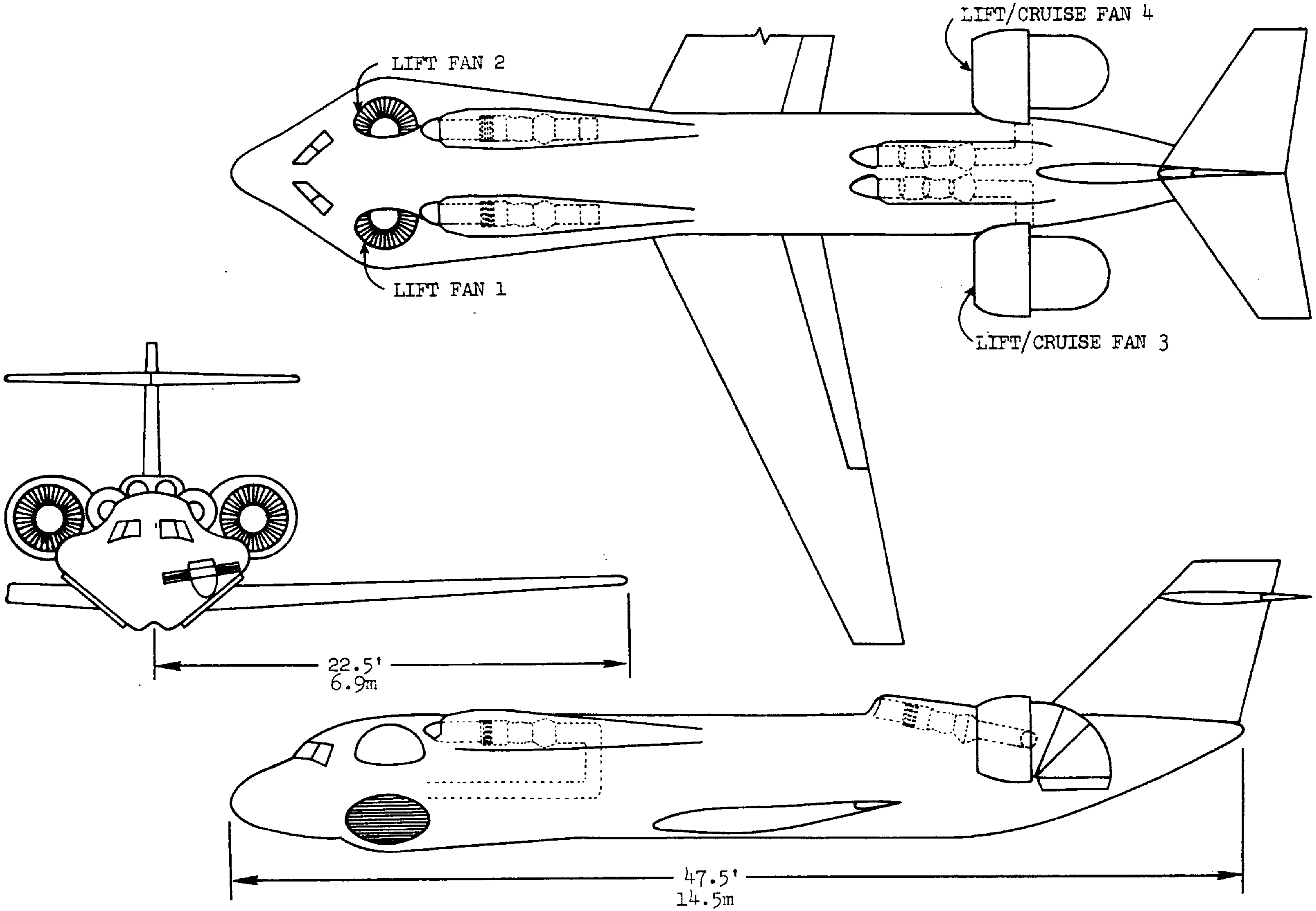

FIGURE 4 V/STOL MODEL TRANSPORT SCHEMATIC

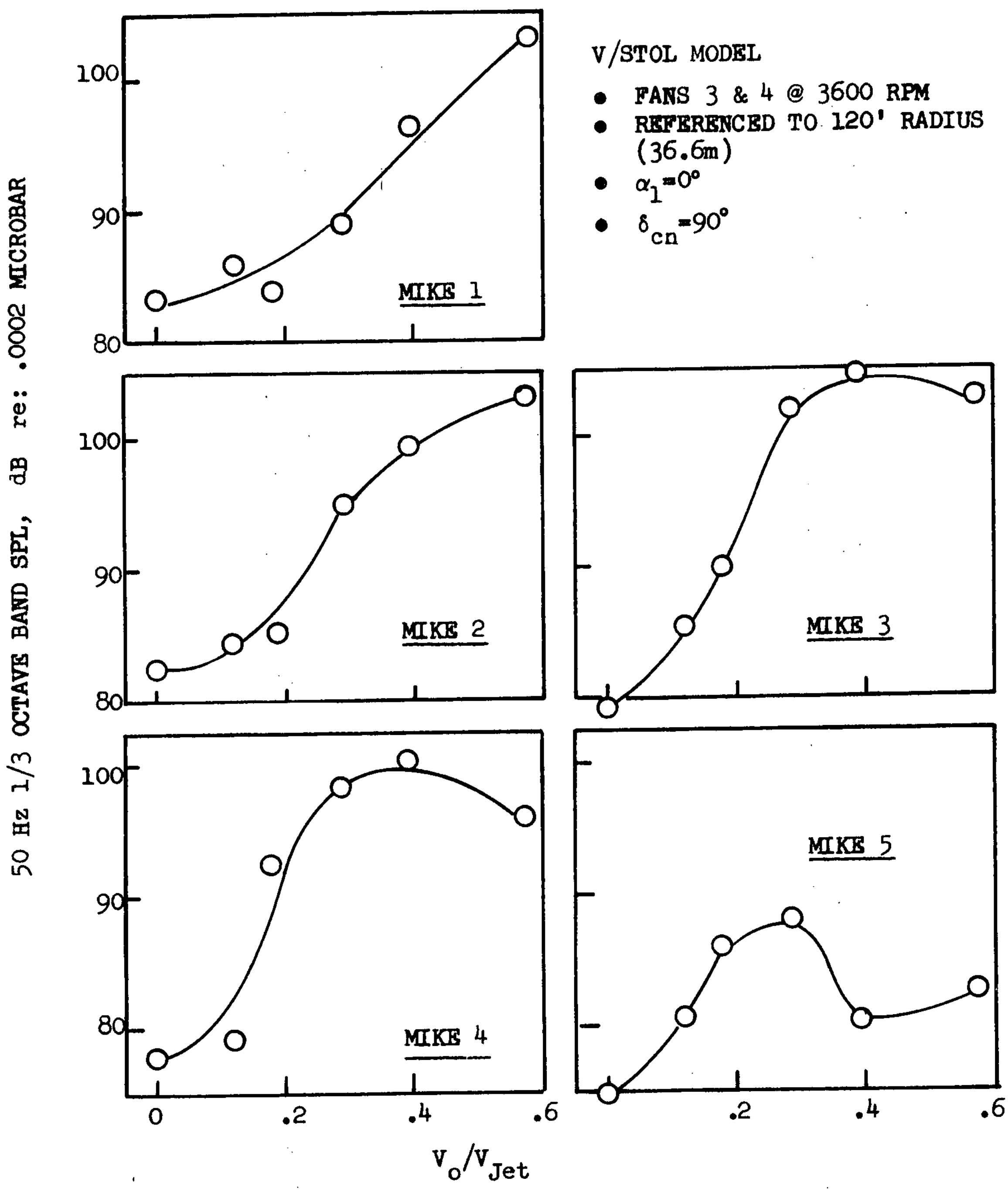

FIGURE 5 EFFECT OF CROSSFLOW ON 50 Hz SPL OF V/STOL MODEL LIFT/CRUISE FANS (DOWNSTREAM MICROPHONES).

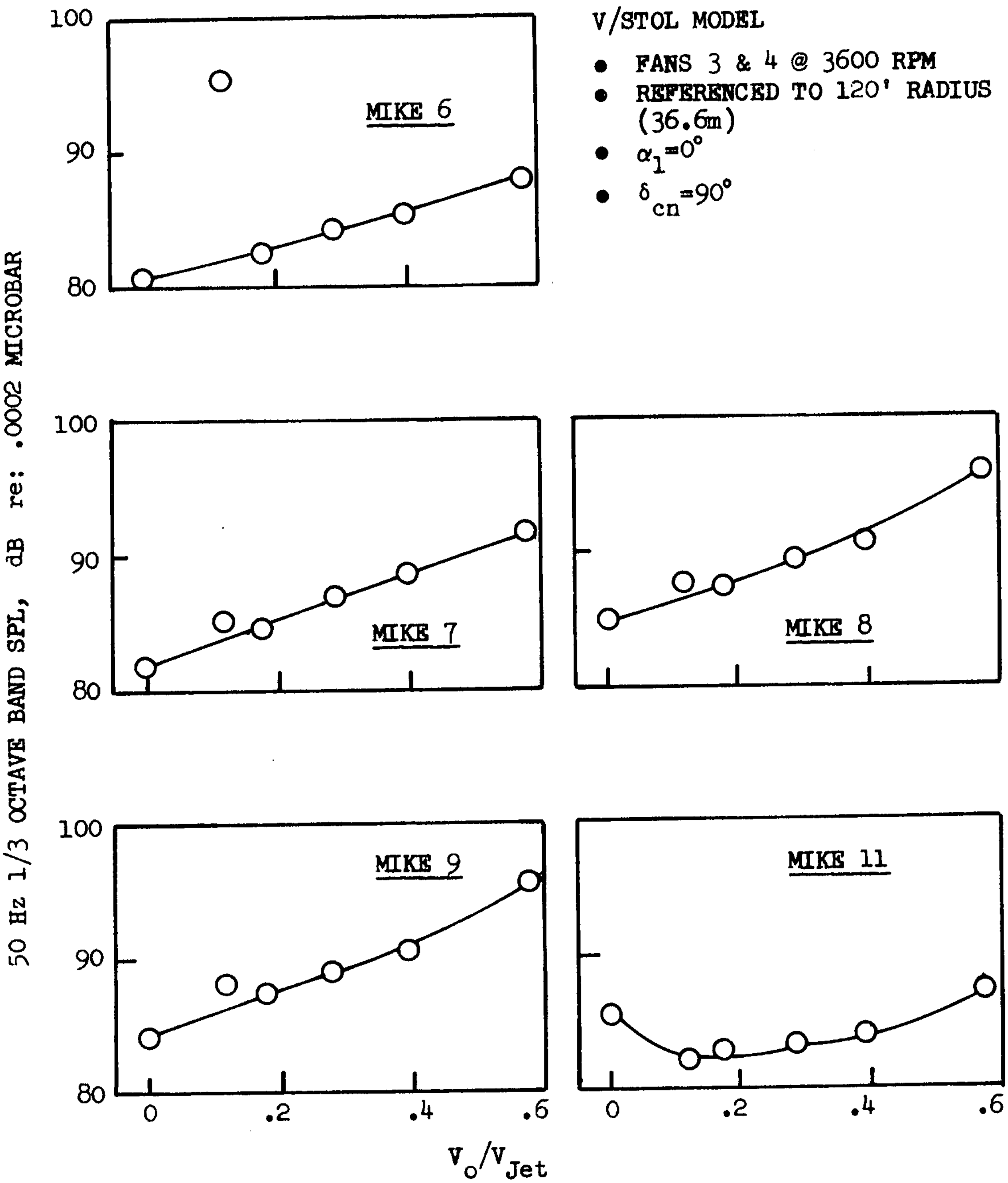

FIGURE 6 EFFECT OF CROSSFLOW ON 50 Hz SPL OF V/STOL MODEL LIFT/CRUISE FANS (UPSTREAM MICROPHONES)

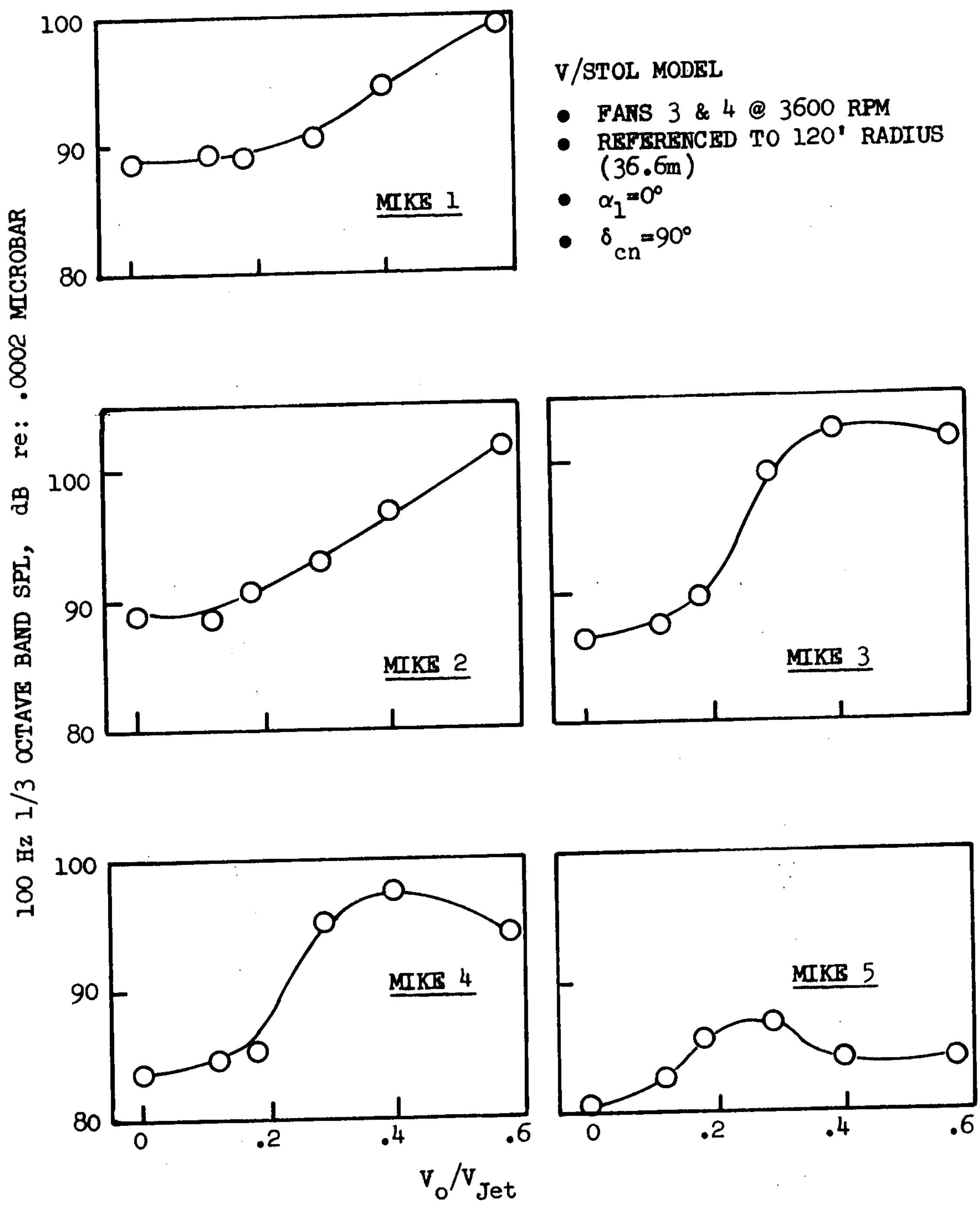

FIGURE 7 EFFECT OF CROSSFLOW ON 100 Hz SPL OF V/STOL MODEL LIFT/CRUISE FANS (DOWNSTREAM MICROPHONES).

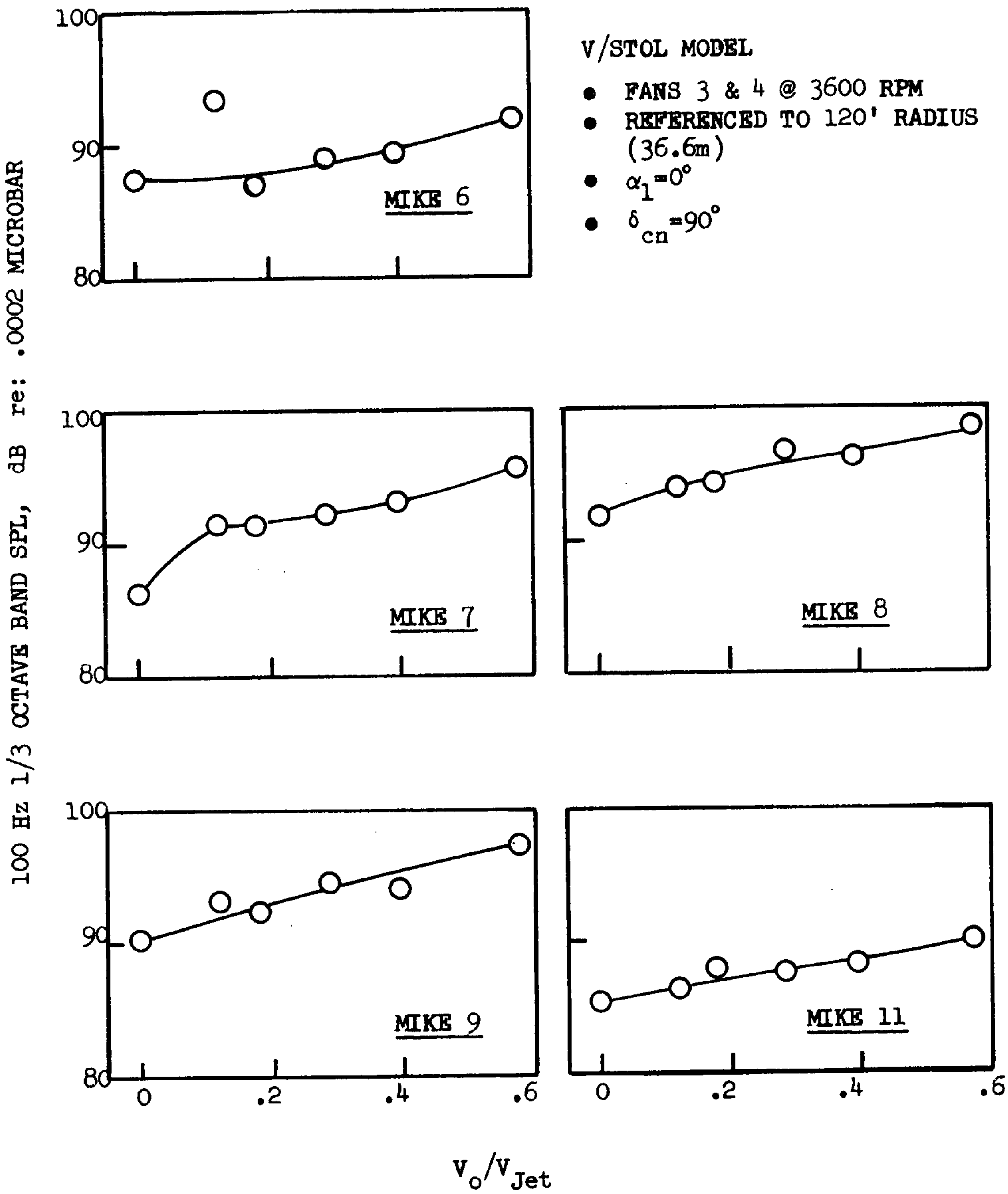

FIGURE 8 EFFECT OF CROSSFLOW ON 100 Hz SPL OF V/STOL MODEL LIFT/CRUISE FANS (UPSTREAM MICROPHONES).

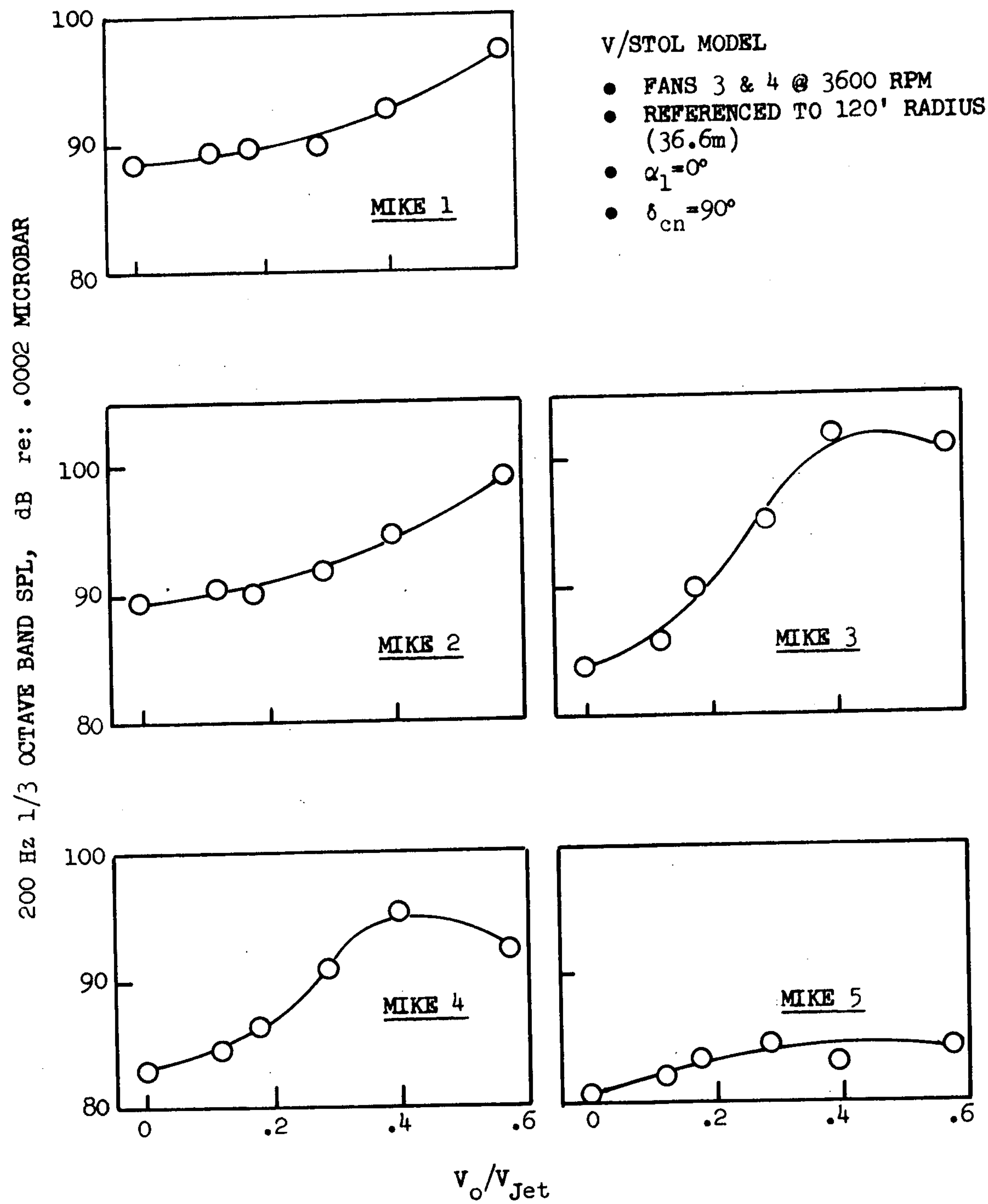

FIGURE 9 EFFECT OF CROSSFLOW ON 200 Hz SPL OF V/STOL MODEL LIFT/CRUISE FANS (DOWNSTREAM MICROPHONES).

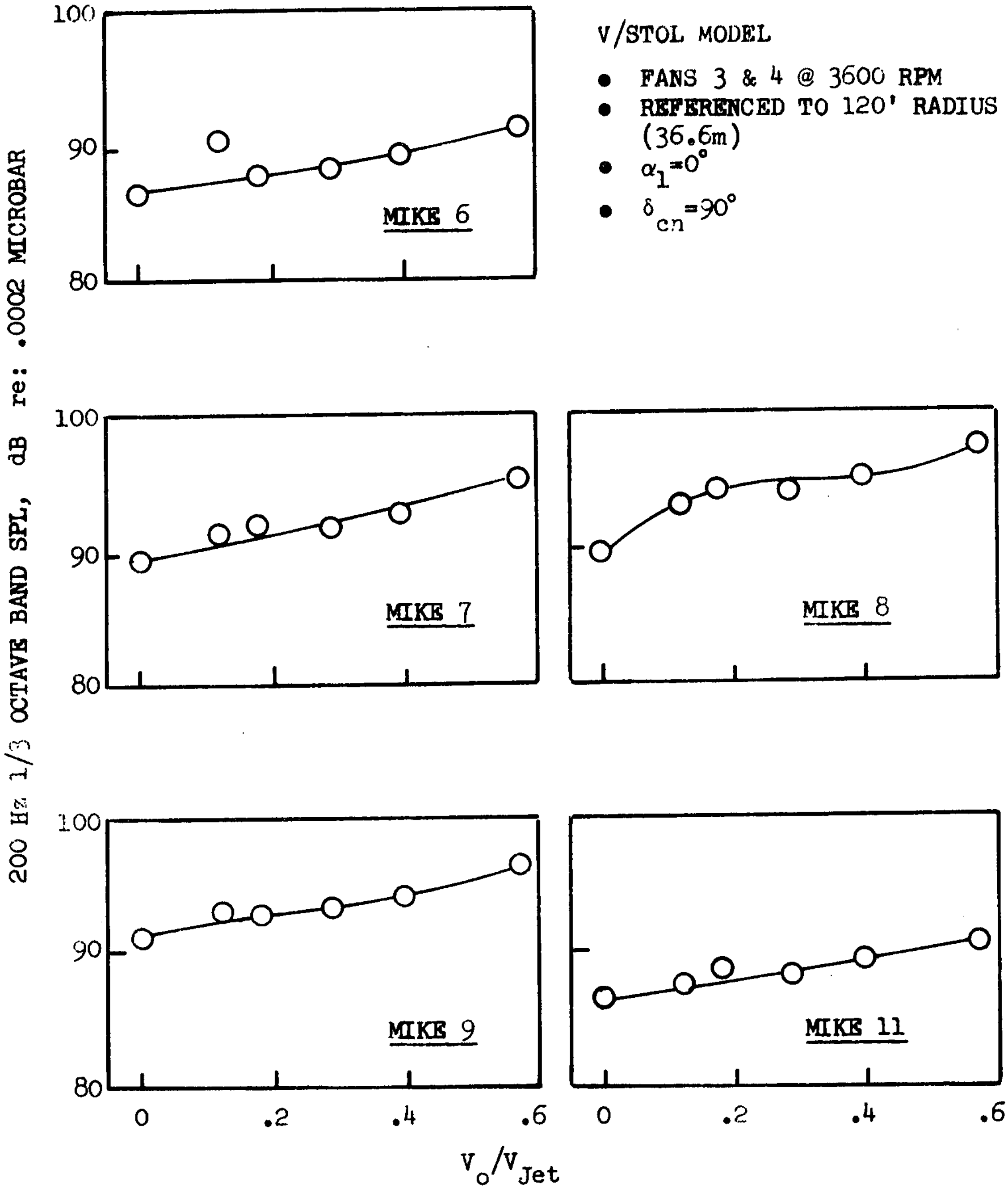

FIGURE 10 EFFECT OF CROSSFLOW ON 200 Hz SPL OF V/STOL MODEL LIFT/CRUISE FANS (UPSTREAM MICROPHONES).

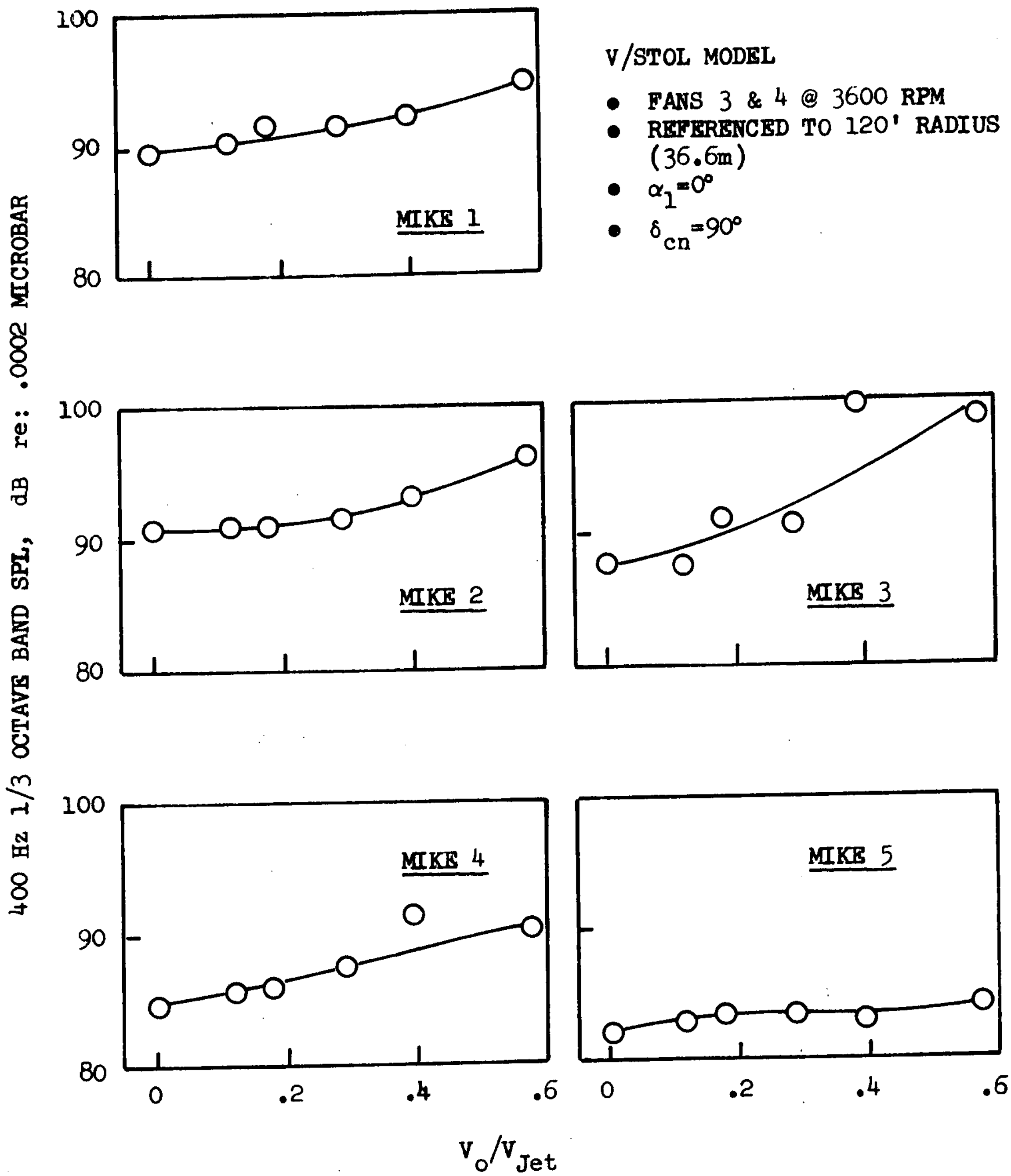

FIGURE 11 EFFECT OF CROSSFLOW ON 400 Hz SPL OF V/STOL MODEL LIFT/CRUISE FANS (DOWNSTREAM MICROPHONES).

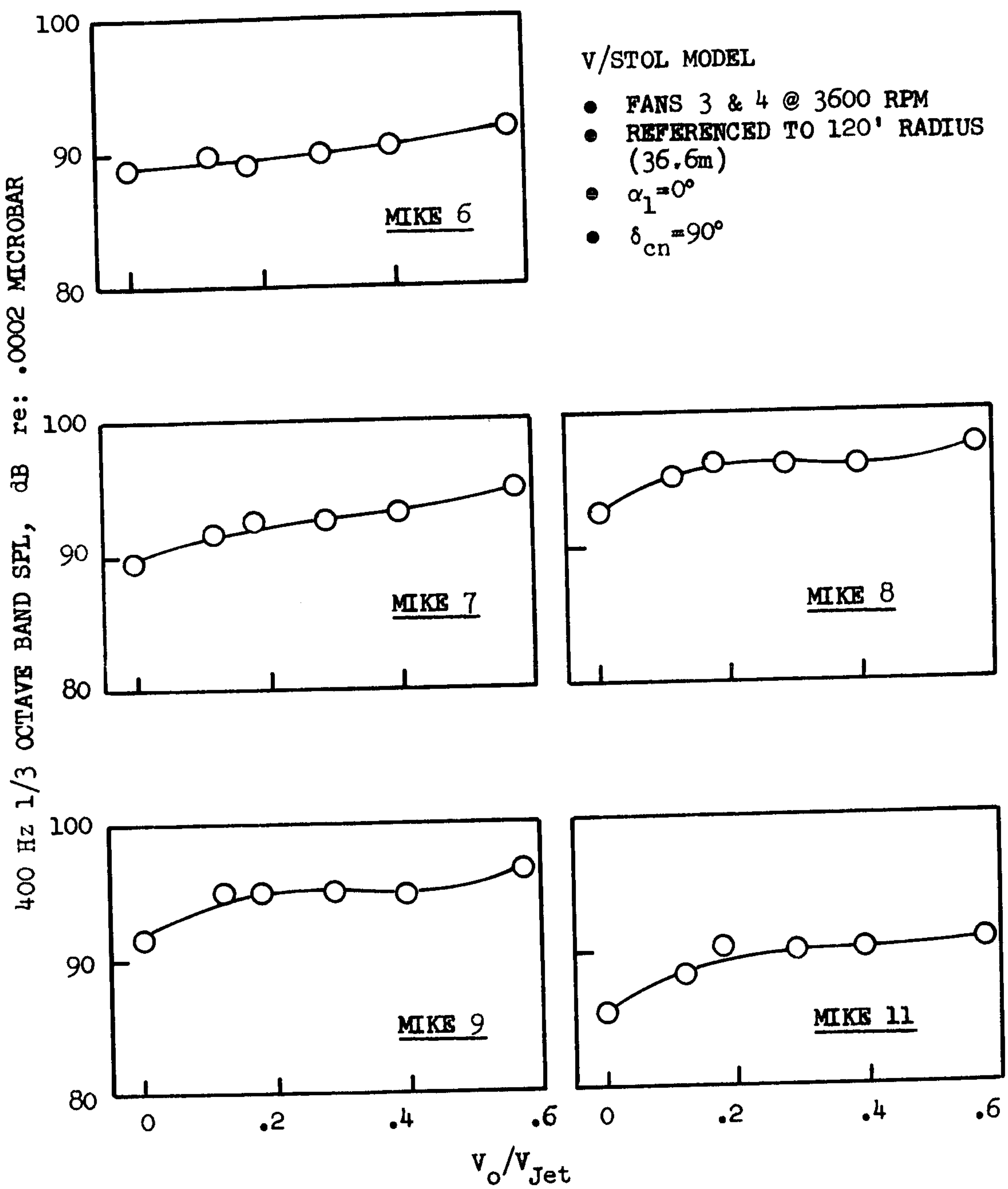

FIGURE 12 EFFECT OF CROSSFLOW ON 400 Hz SPL OF V/STOL MODEL LIFT/CRUISE FANS (UPSTREAM MICROPHONES).

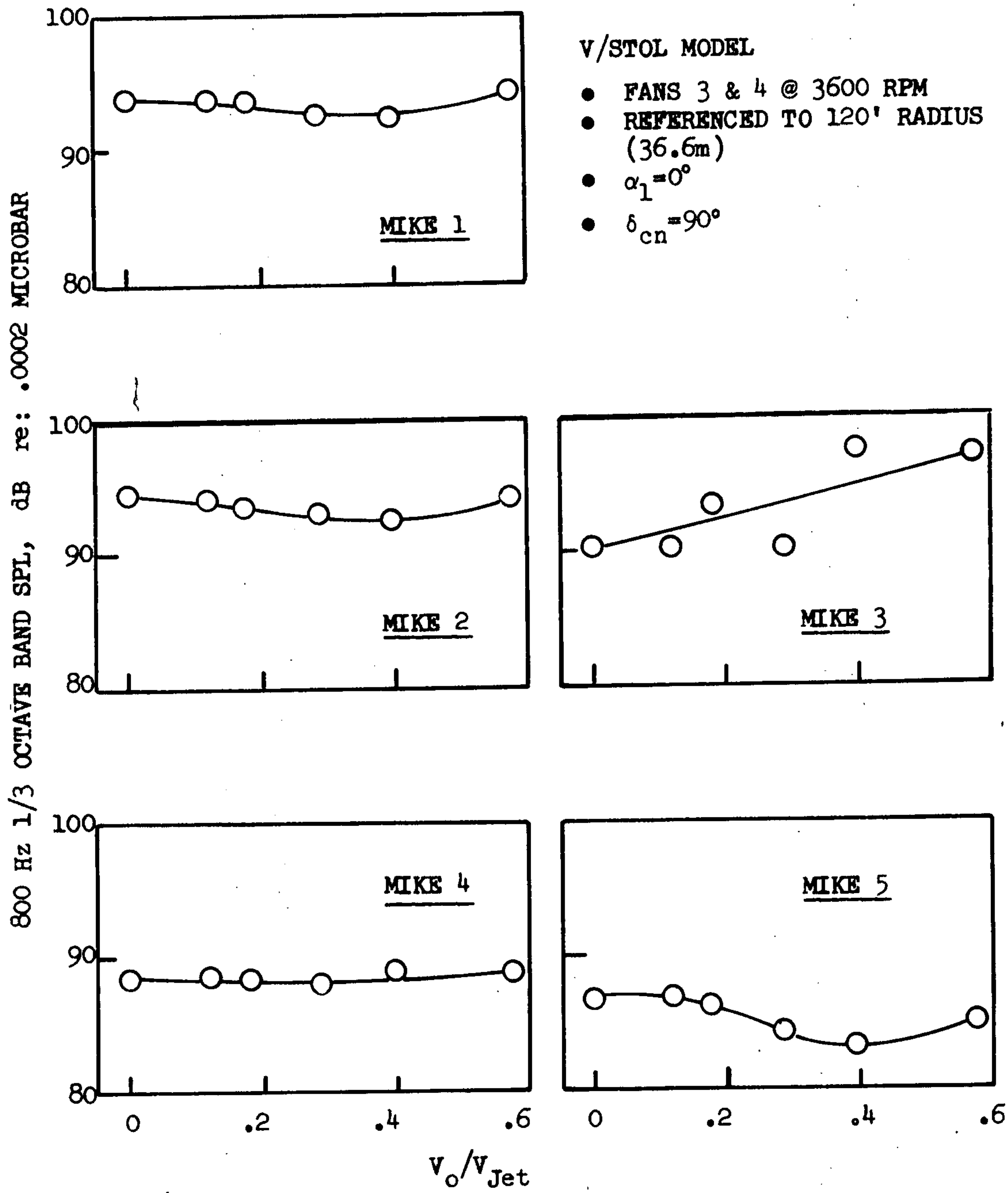

FIGURE 13 EFFECT OF CROSSFLOW ON 800 Hz SPL OF V/STOL MODEL LIFT/CRUISE FANS (DOWNSTREAM MICROPHONES).

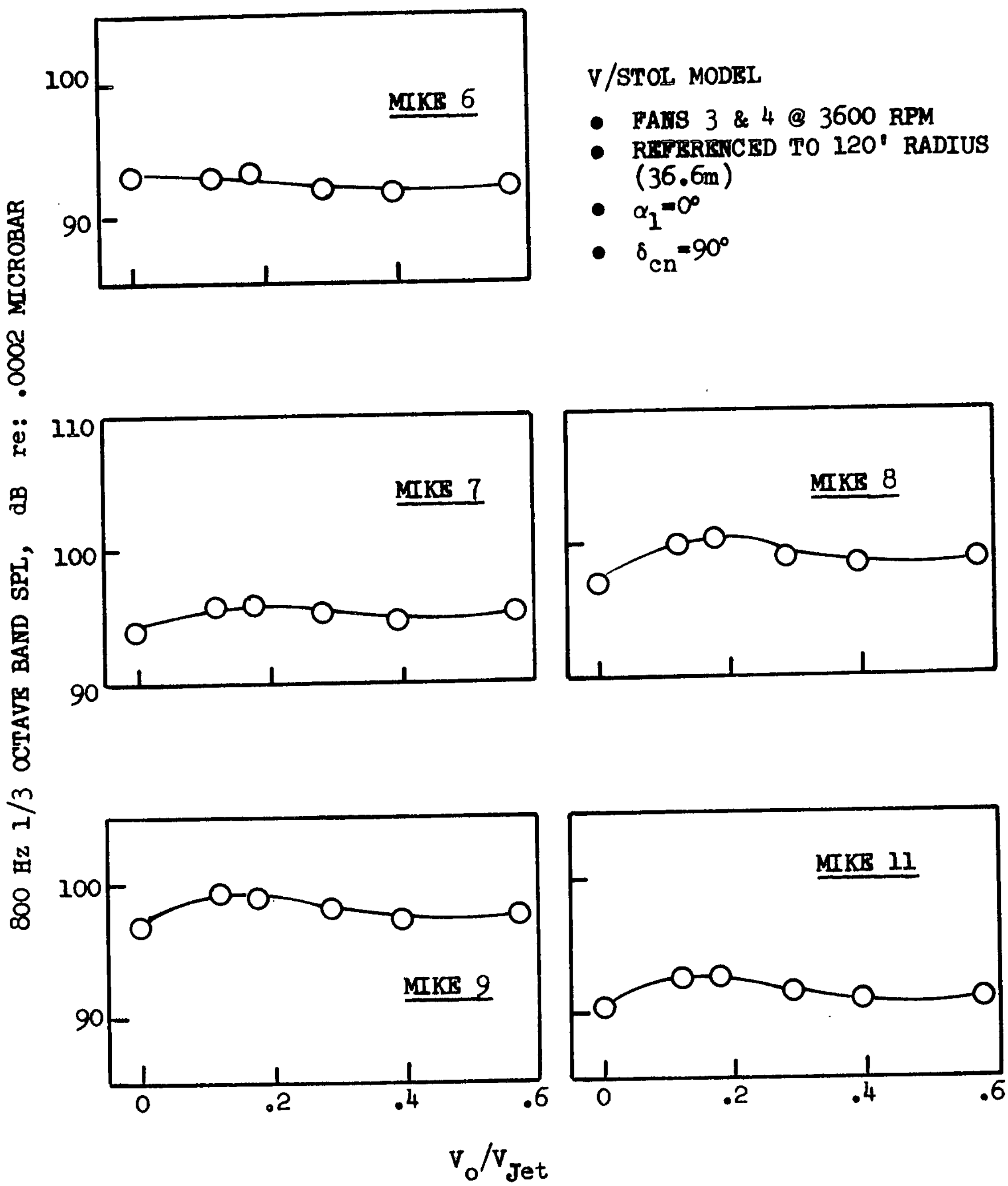

FIGURE 14 EFFECT OF CROSSFLOW ON 800 Hz SPL OF V/STOL MODEL LIFT/CRUISE FANS (UPSTREAM MICROPHONES).

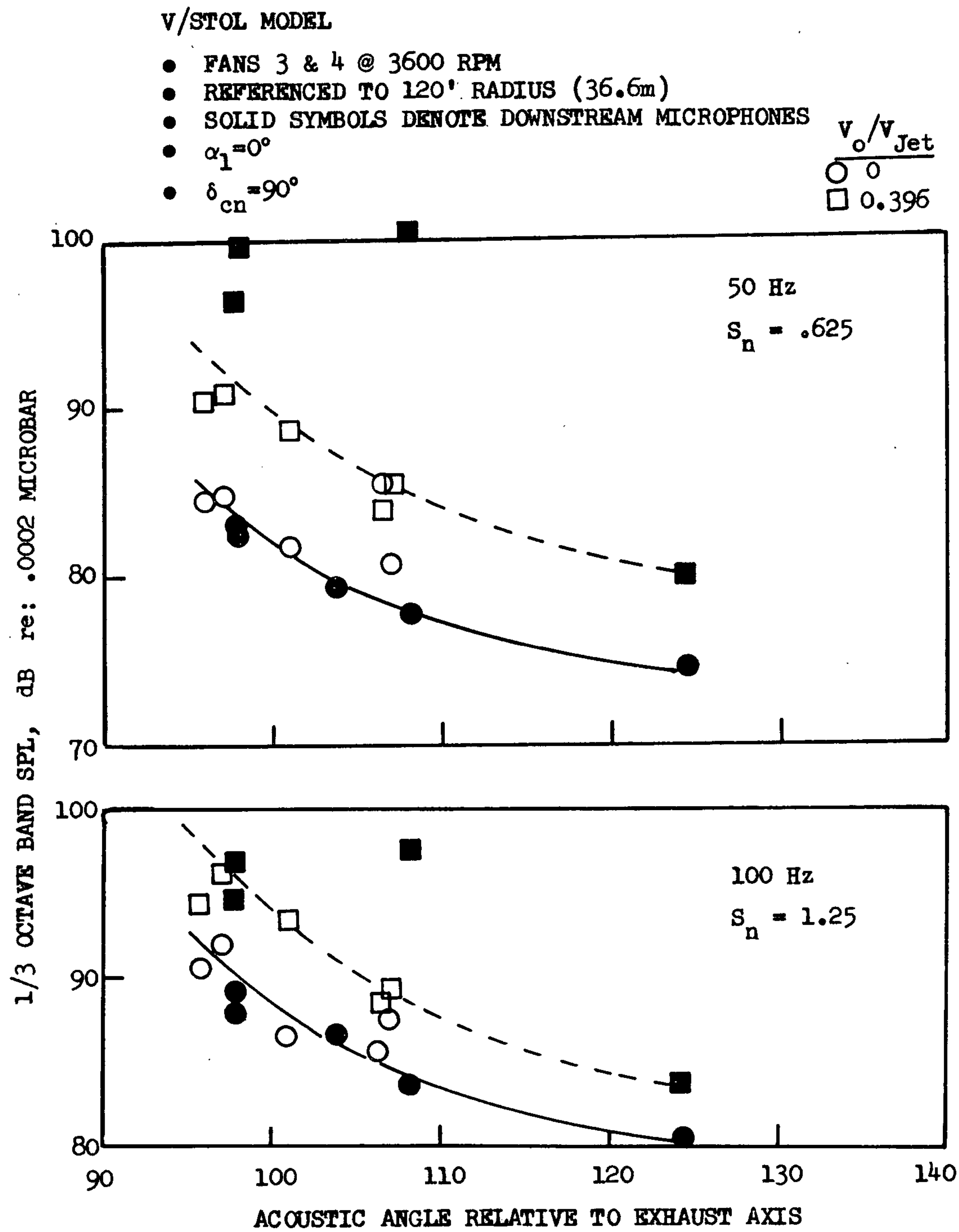

FIGURE 15 V/STOL MODEL LIFT/CRUISE FAN JET NOISE DIRECTIVITY PATTERN AT V_o/V_{JET} = 0 and 0.396.

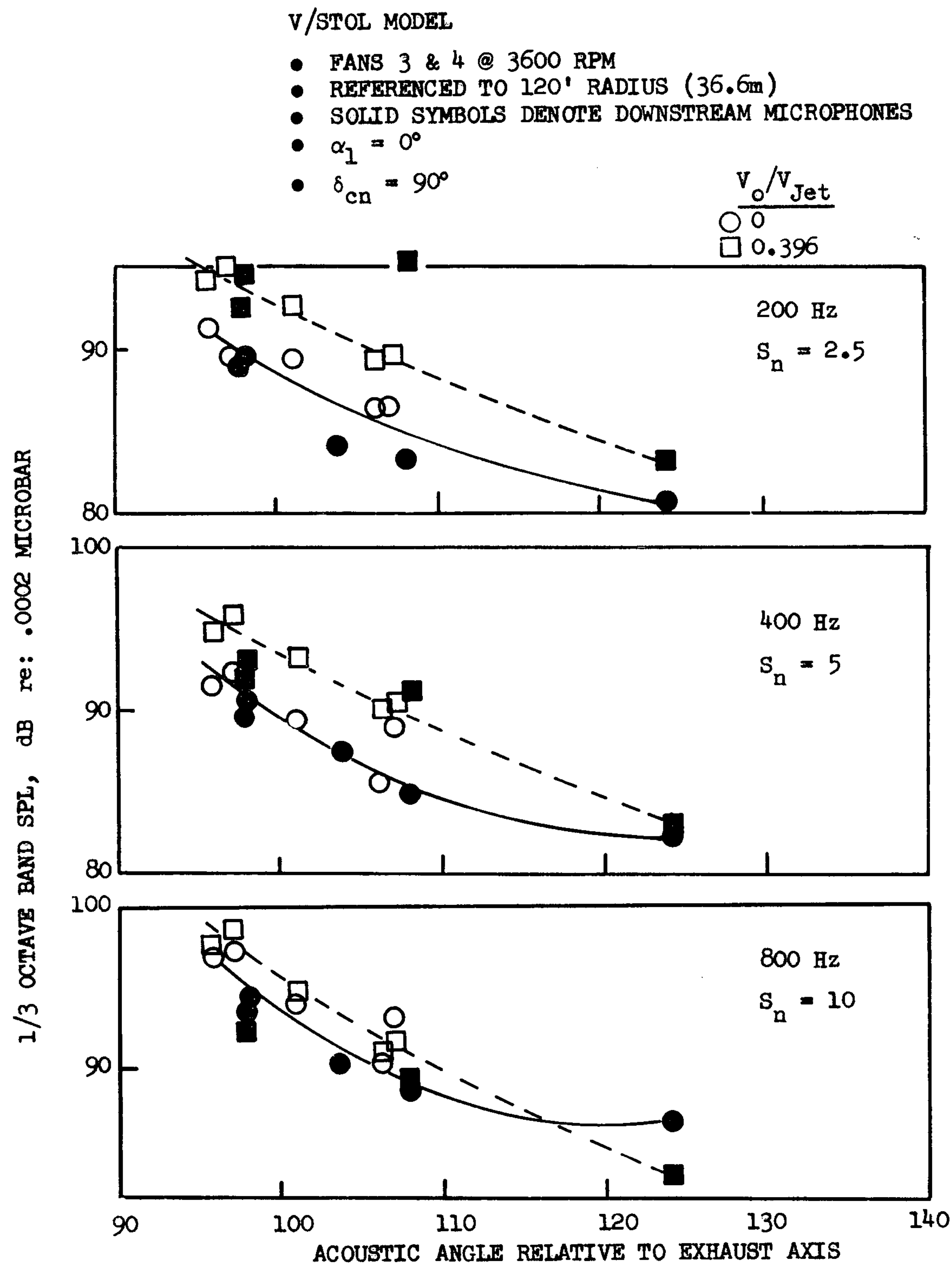

FIGURE 16 V/STOL MODEL LIFT/CRUISE FAN JET NOISE DIRECTIVITY PATTERN AT V_o/V_{JET} = 0 AND 0.396 .

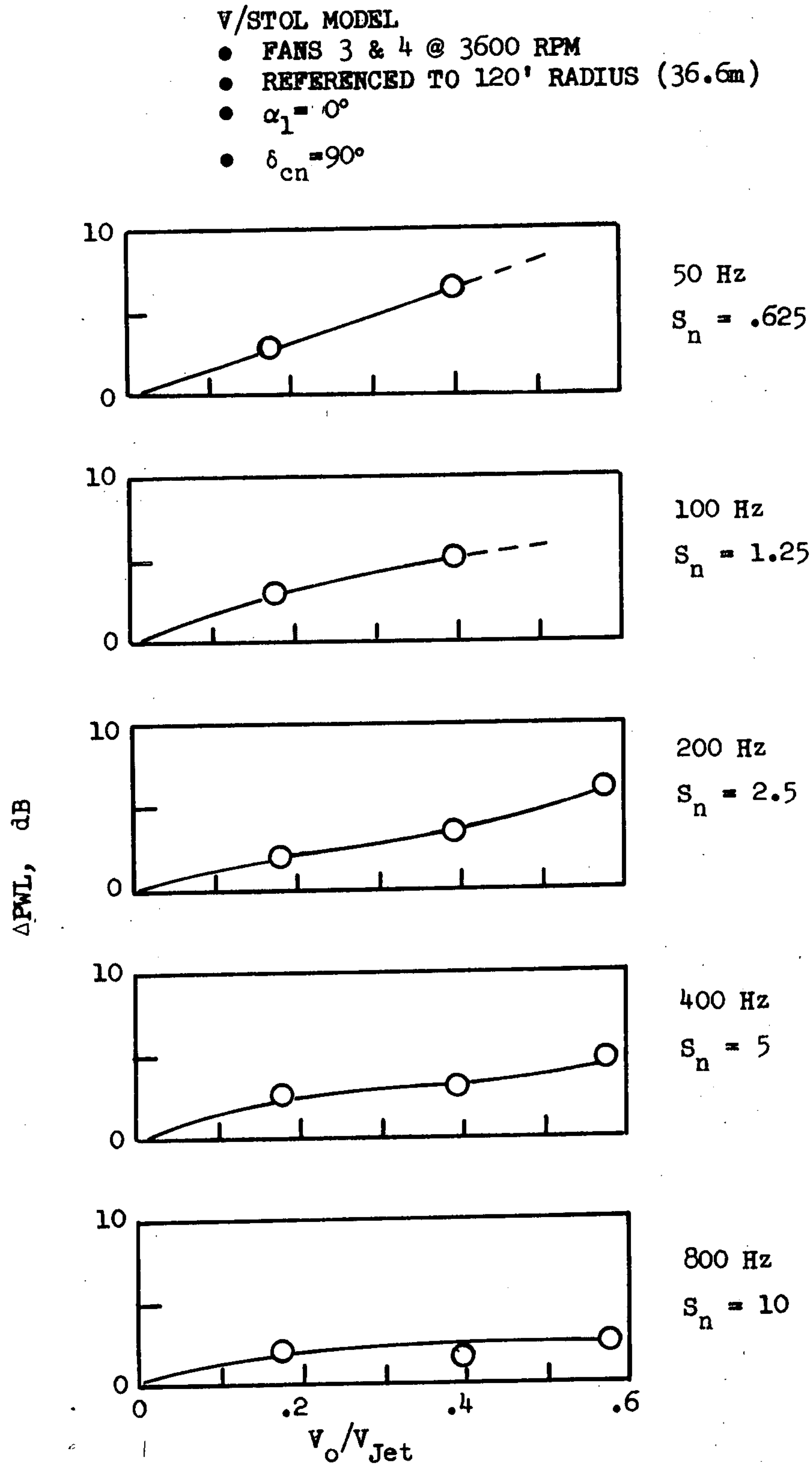

FIGURE 17 JET NOISE LEVEL INCREASE WITH INCREASED CROSSFLOW AT VARIOUS STROUHAL NUMBERS.

- LIFT/CRUISE FANS @ 3600 RPM
- $\delta_{cn}=90°$
- $\alpha_1=\beta_v=\sigma_v=0°$

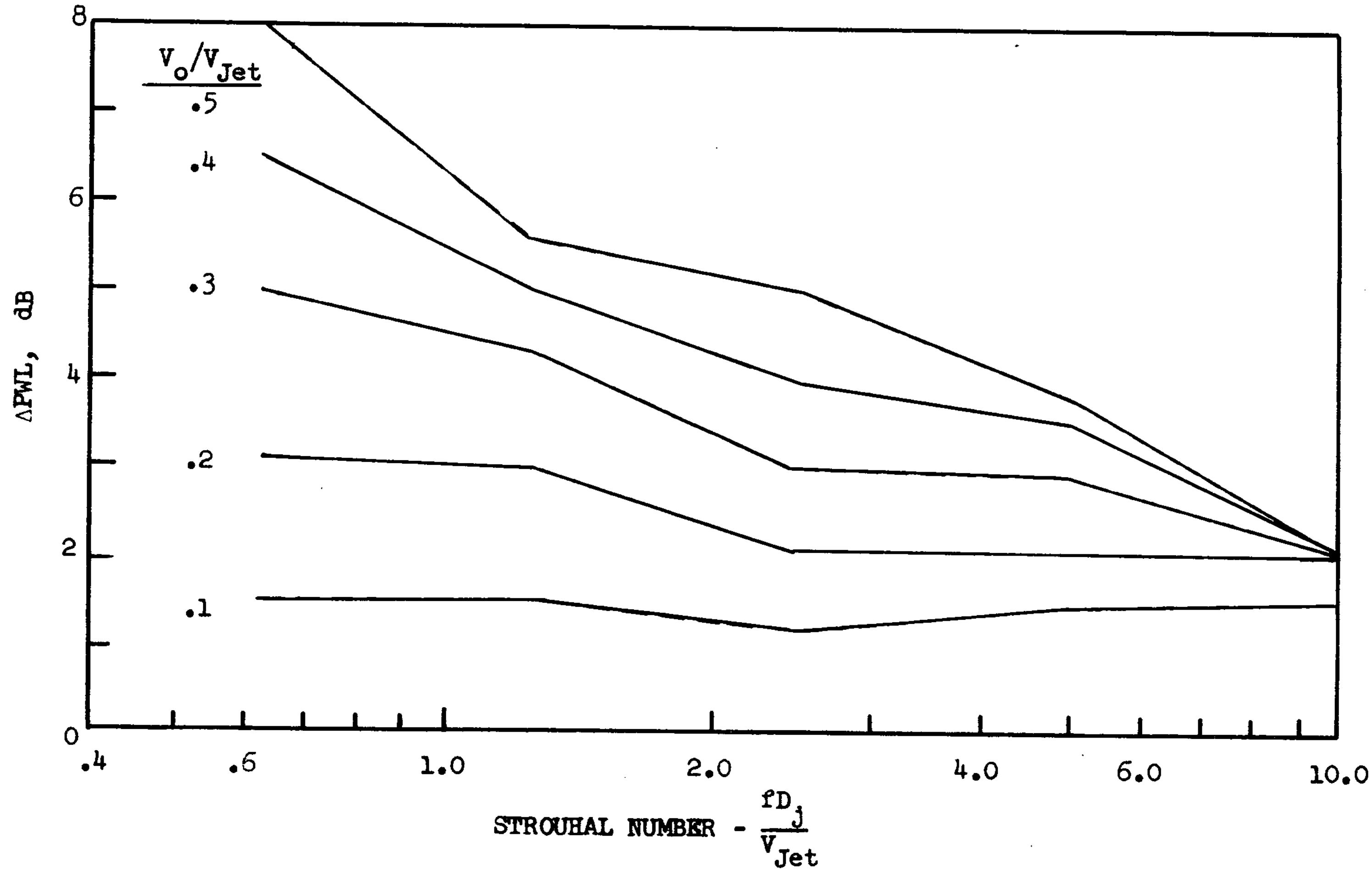

FIGURE 18 JET NOISE POWER LEVEL CHANGE AS A FUNCTION OF STROUHAL NUMBER FOR VARIOUS CROSSFLOW VELOCITY RATIOS.

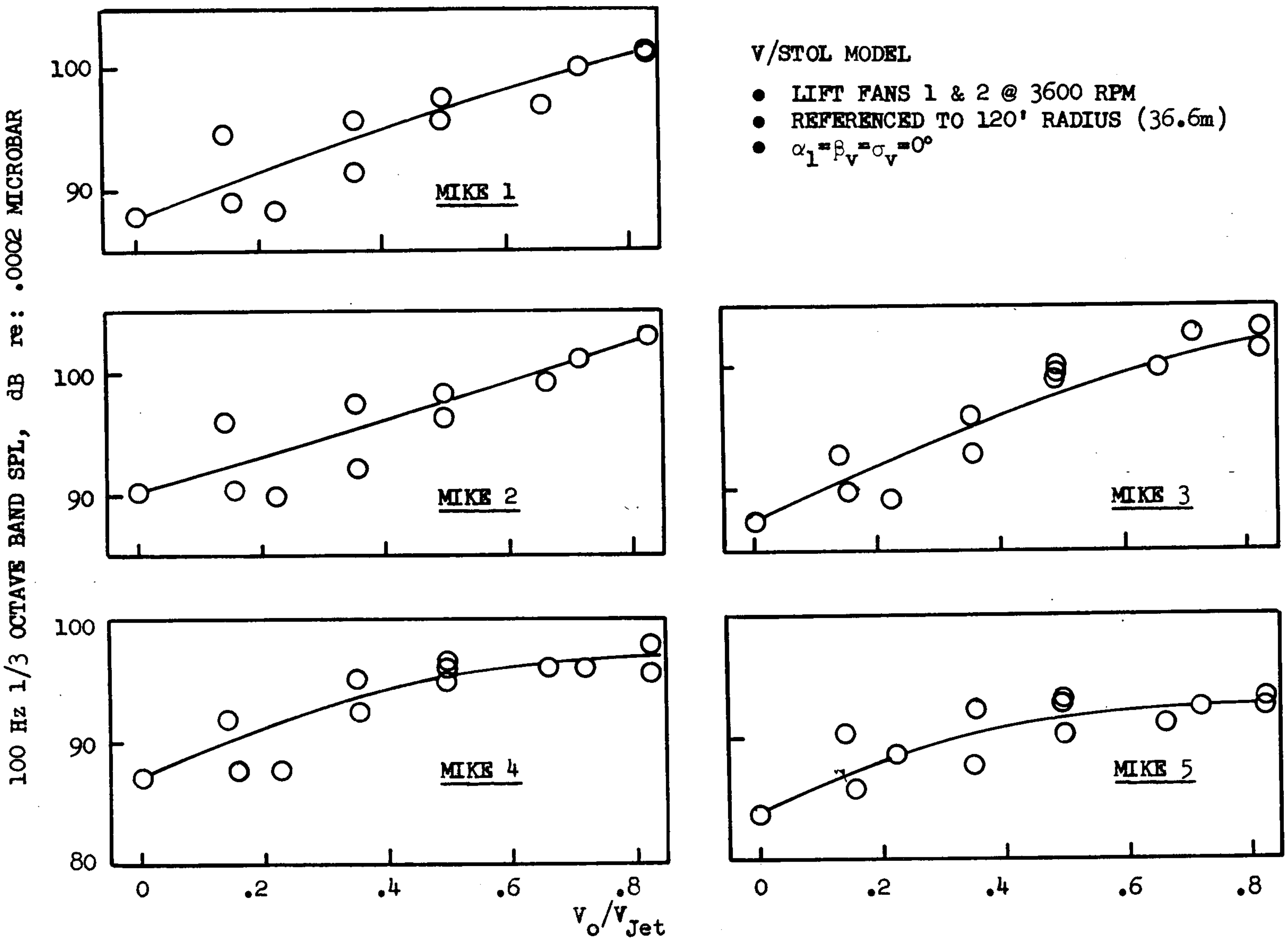

FIGURE 19 EFFECT OF CROSSFLOW ON 100 Hz SIGNAL FROM V/STOL MODEL LIFT FANS (DOWNSTREAM MICROPHONES).

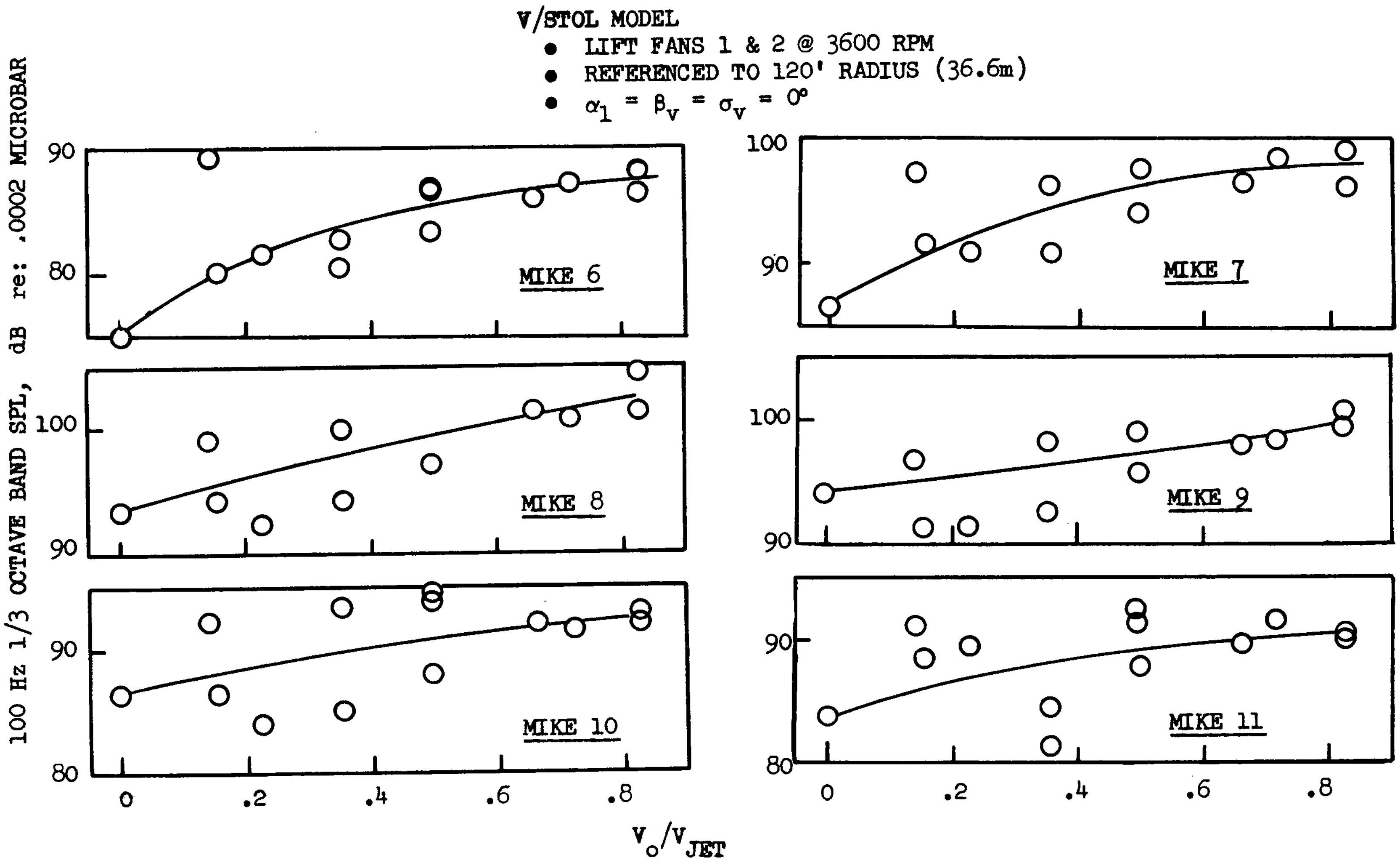

FIGURE 20 EFFECT OF CROSSFLOW ON 100 Hz SIGNAL FROM V/STOL MODEL LIFT FANS (UPSTREAM MICROPHONES).

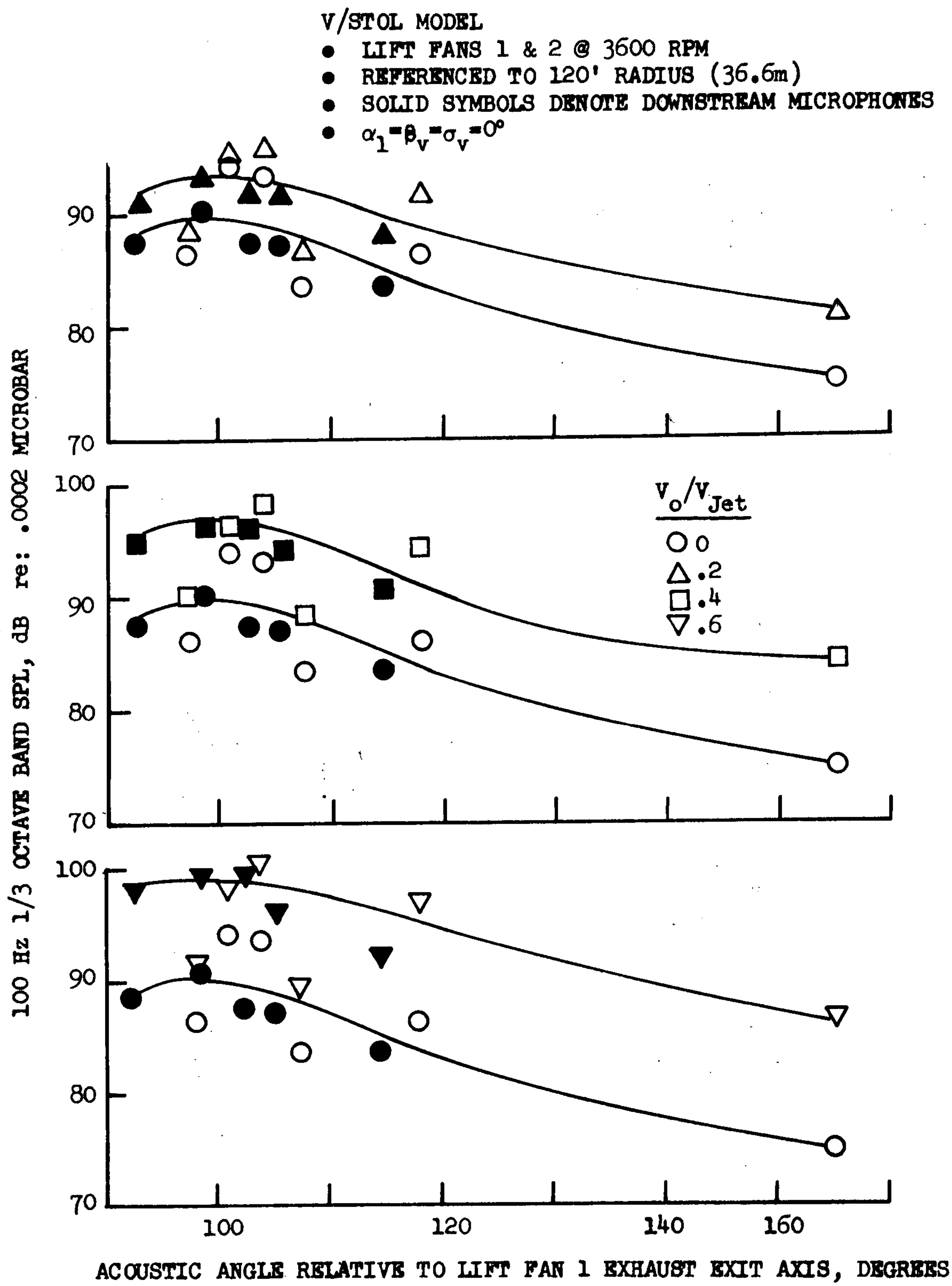

FIGURE 21 V/STOL MODEL LIFT FAN JET NOISE DIRECTIVITY PATTERN AT 100 Hz

V/STOL MODEL

- LIFT FANS 1 & 2 @ 3600 RPM
- $\alpha_1 = \beta_v = \sigma_v = 0°$
- $\delta_{cn} = 90°$

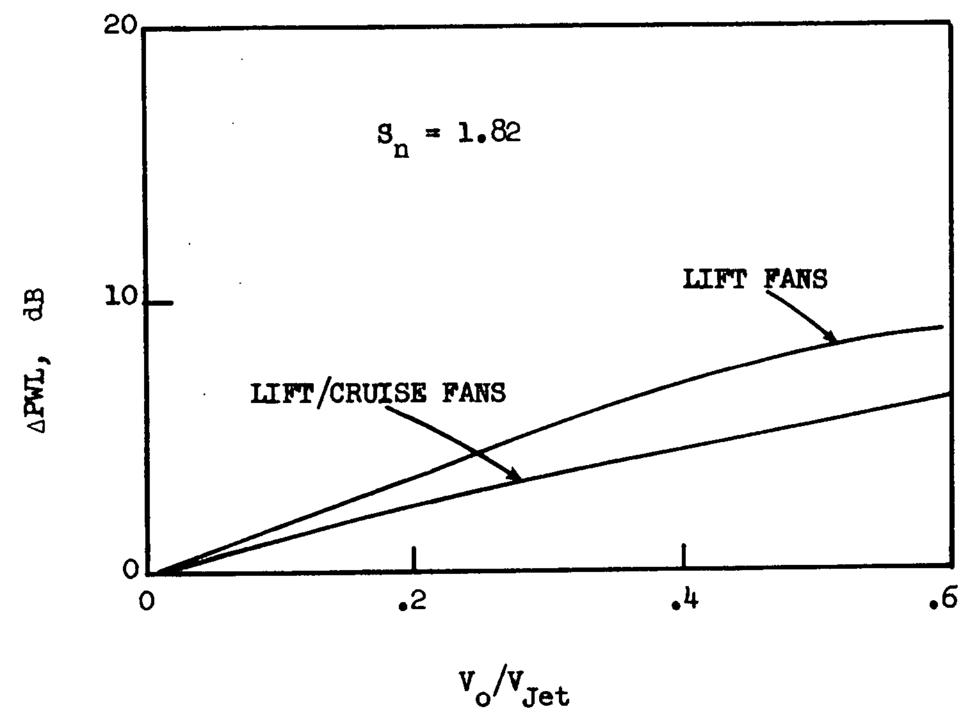

FIGURE 22 COMPARISON OF CROSSFLOW EFFECT ON JET NOISE POWER LEVEL OF V/STOL MODEL LIFT FANS AND LIFT/CRUISE FANS.

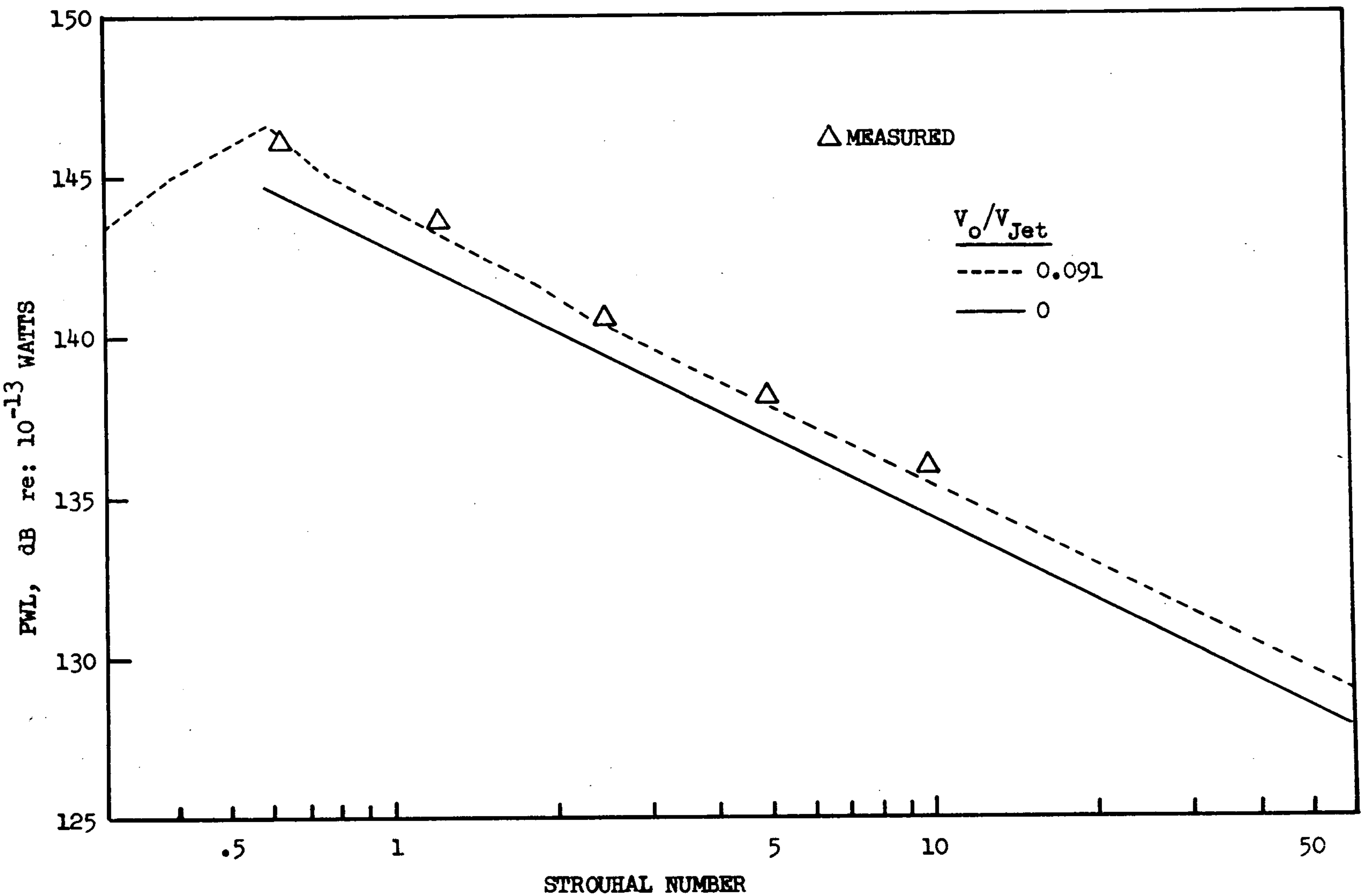

FIGURE 23 COMPARISON OF MEASURED AND PREDICTED POWER SPECTRA AT V_o/V_{JET} = 0.091

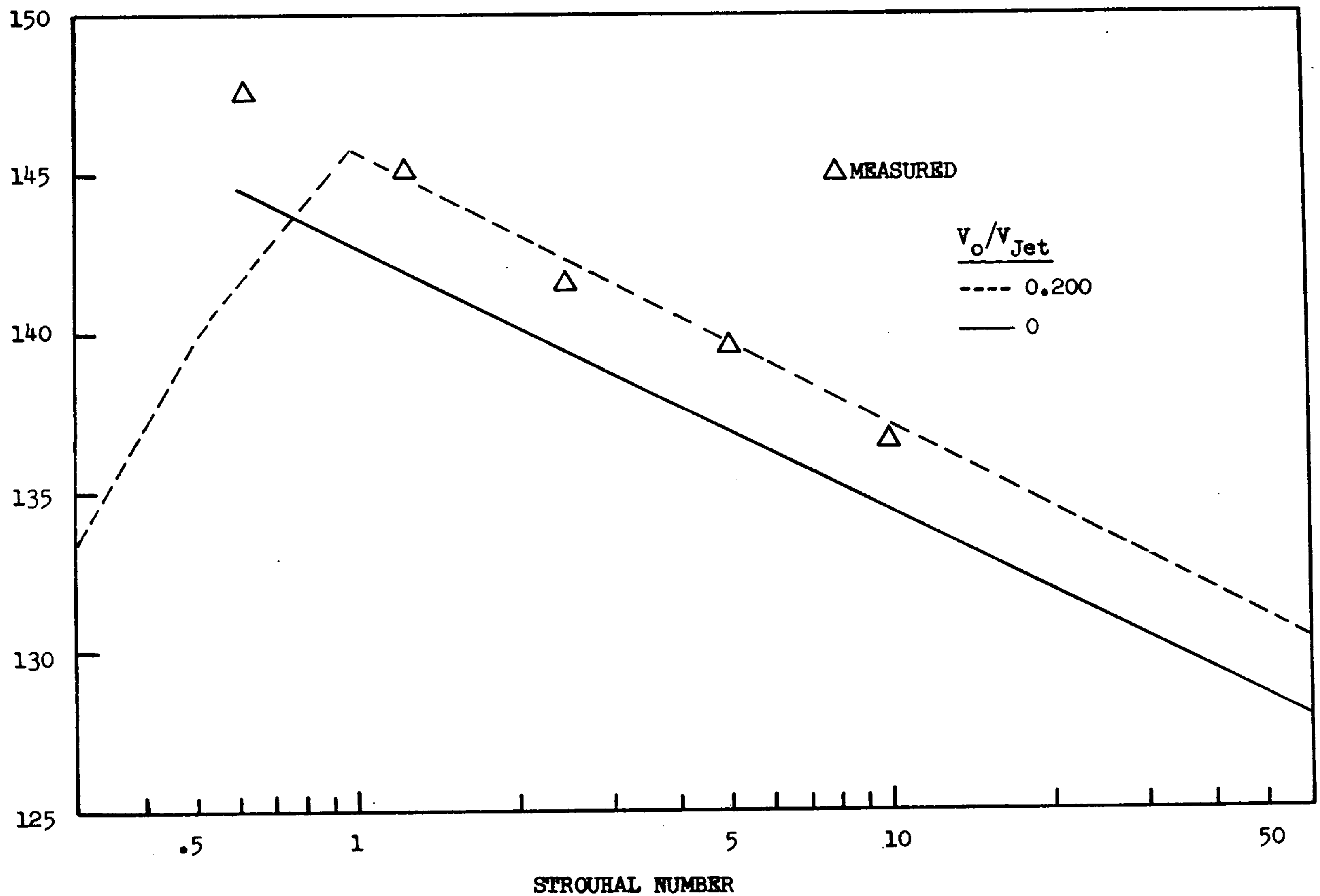

FIGURE 24 COMPARISON OF MEASURED AND PREDICTED POWER SPECTRA AT V_o/V_{JET} = 0.2

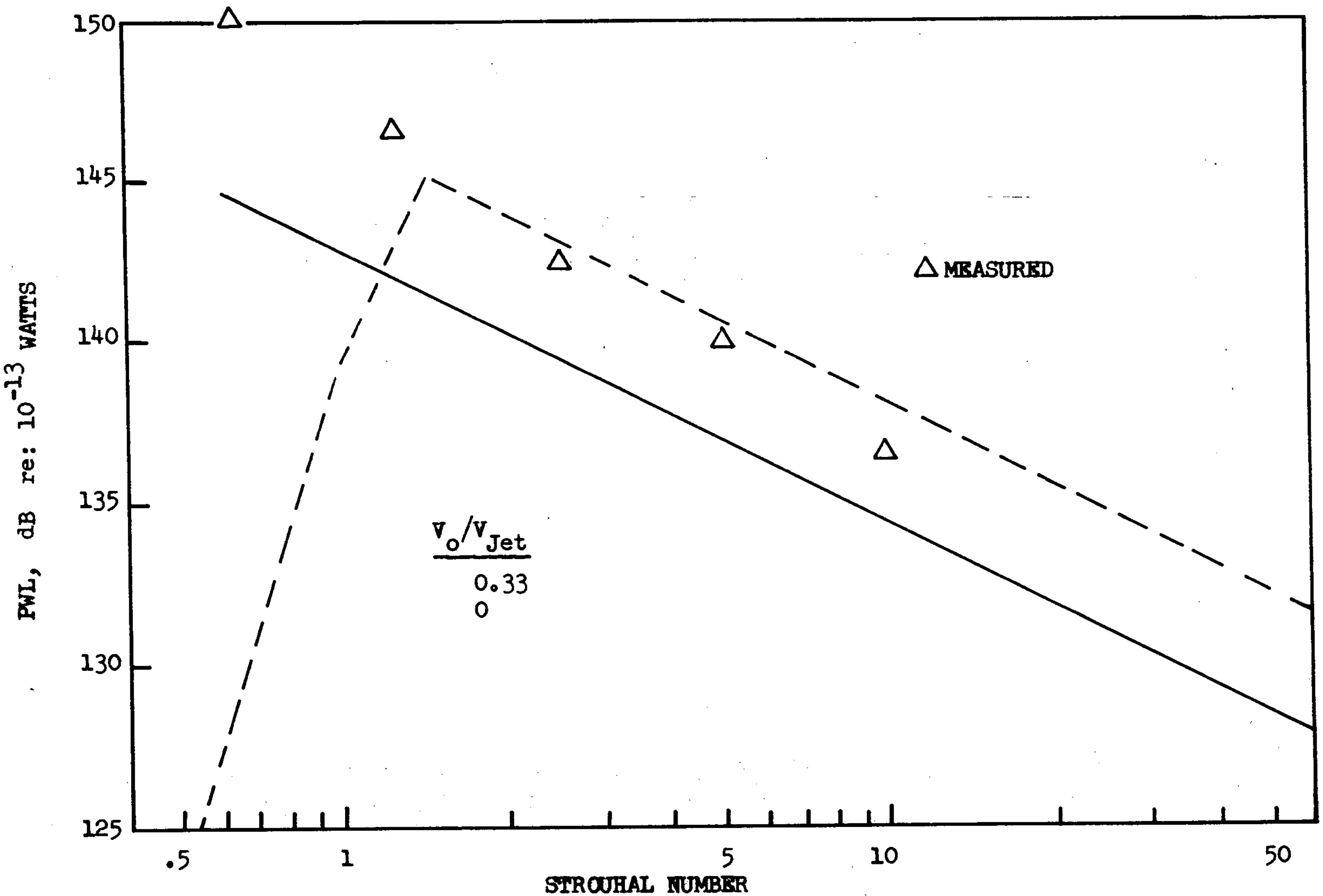

FIGURE 25 COMPARISON OF MEASURED AND PREDICTED POWER SPECTRA AT V_o/V_{JET} = 0.33

REFERENCES

1. Kirk, J.V., Hall, L.P., and Hodder, B.K., "Aerodynamics of Lift Fan V/STOL Aircraft," NASA TM X-62, 086, September 1971.

2. "Jet Noise Prediction," Aerospace Information Report 876, Society of Automotive Engineers, Inc., July 10, 1965

3. Lee, R., et al, "Research Investigation of the Generation and Suppression of Jet Noise," General Electric Flight Propulsion Division, Prepared under Bureau of Naval Weapons, Contract #NOas 59-6160-C, June 1961.

4. NASA Report #1338, "Near Field Noise of a Jet Engine Exhaust."

5. Bowley, W.W., and Sucec, J., "Trajectory and Spreading of a Turbulent Jet in the Presence of a Crossflow of Arbitrary Velocity Distribution," ASME Paper presented at Gas Turbine Conference & Products Show,. Cleveland, Ohio, March 9 - 13, 1969.

6. Hickey, D.H., Soderman, P.T., and Kelly, M.W., "Noise Measurements in Wind Tunnels," pp. 399-408, Basic Aerodynamic Noise Research, NASA SP-207, July 14, 1969.

7. Stimpert, D.L., "Effect of Crossflow Velocity on VTOL Lift Fan Blade Passing Frequency Noise Generation," NASA CR 114566, February 1973.